Calhoun: The NPS Institutional Archive

DSpace Repository

Theses and Dissertations	1. Thesis and Dissertation Collection, all items

1946-09

Turbulent mixing along the boundaries of parallel flow streams

Naymark, Sherman; Kintner, Edwin Earl; Naymark, Sherman; Kintner, Edwin Earl

Massachusetts Institute of Technology

http://hdl.handle.net/10945/6603

This publication is a work of the U.S. Government as defined in Title 17, United States Code, Section 101. Copyright protection is not available for this work in the United States.

Downloaded from NPS Archive: Calhoun

http://www.nps.edu/library

Calhoun is the Naval Postgraduate School's public access digital repository for research materials and institutional publications created by the NPS community. Calhoun is named for Professor of Mathematics Guy K. Calhoun, NPS's first appointed -- and published -- scholarly author.

Dudley Knox Library / Naval Postgraduate School
411 Dyer Road / 1 University Circle
Monterey, California USA 93943

TURBULENT MIXING ALONG THE BOUNDARIES OF PARALLEL FLOW STREAMS

SHERMAN NAYMARK
EDWIN EARL KINTNER

Library
U. S. Naval Postgraduate School
Monterey, California

Mont. 132
895k

COPY FOR HEAD OF POSTGRADUATE SCHOOL

MASSACHUSETTS INSTITUTE OF TECHNOLOGY
Department of Mechanical Engineering
Cambridge 39, Mass., U.S.A.

Room 1-202

September 24, 1946

Captain W. H. Buracker
Room 5-233
Massachusetts Institute of Technology
Cambridge 39, Massachusetts

Thesis Work of LCDR E.E. KINTNER, USN
LCDR S. NAYMARK, USN

Dear Captain Buracker:

This is in reply to your request for an appraisal of the work done by Lt. Comdr. E. E. Kintner and Lt. Comdr. S. Naymark on their thesis research.

These men made a fundamental study of the mechanism of mixing of two parallel gas streams. The results they obtained were hitherto not available, and will doubtless find application in the design of combustion chambers, jet pumps, and jet propulsion devices.

It may be of interest to you to know that this research program is considered of sufficient importance to warrant its continuation and enlargement under the sponsorship of Project Meteor.

Very sincerely yours,

/s/ Ascher H. Shapiro

Ascher H. Shapiro

6

TURBULENT MIXING ALONG THE BOUNDARIES OF PARALLEL FLOW STREAMS

by

SHERMAN NAYMARK
Lieutenant Commander, U.S.N.

and

EDWIN E. KINTNER
Lieutenant Commander, U.S.N.

Submitted in Partial Fulfillment

of the Requirements for the Degree of

Master of Science in Naval Construction and Engineering

from the

Massachusetts Institute of Technology

1946

Cambridge, Massachusetts,
September 16, 1946.

Professor J. S. Newell
Secretary of the Faculty,
Massachusetts Institute of Technology,
Cambridge, Massachusetts.

Dear Sir:

In accordance with the requirements for the Degree of Master of Science in Naval Construction and Engineering, we submit herewith a thesis entitled, "Turbulent Mixing Along the Boundaries of Parallel Flow Streams."

ACKNOWLEDGEMENT

The authors wish to express their appreciation to Commander Bennett C. Oelheim, U.S.N., and Commander Robert A. Thacher, U.S.N. for use of their equipment and advice, to Professors G. B. Wilkes and L. R. Vianey for the use of their equipment, and to Professor Ascher H. Shapiro under whose guidance the thesis was conducted.

TABLE OF CONTENTS

CHAPTER	TITLE	PAGE
I	Summary	1
II	Introduction	3
III	Description of Concentration Measuring Apparatus	5
IV	Calibration of Thermal Conductivity Cell Apparatus	11
V	Results of Thermal Conductivity Cell ~~Apparatus~~ Calibration	15
VI	Description of Apparatus and Procedure	21
VII	Results	26
VIII	Discussion of Results	45
IX	Conclusions	51
X	Recommendations	52
XI	Appendix	
	A. Flow Accountability	53
	B. Data Sheets and Sample Calculations	58
	C. References	71

SYMBOLS

x	distance from point of mixing along jet axis (inches)
R	radial distance from jet axis (inches)
a	radius of jet at mixing point (inches)
r_o	radius of outer boundary of jet (inches)
r_i	radius of inner boundary of mixing region (inches)
V_1	velocity of jet leaving nozzle (ft./ sec.)
V_2	velocity of fluid in annulus (stream) (ft./ sec.)
V_o	excess velocity on jet axis over stream velocity (ft./sec.)
V	velocity at any point in 3" pipe (ft./ sec.)
C	Hydrogen concentration at any point in 3" pipe (%)
C_1	hydrogen concentration in jet nozzle (%)

$$\lambda = \frac{V_2}{V_1}$$

CHAPTER I

Summary

A. Object

The object of this investigation was to experimentally determine the manner and rate of mixing along the boundaries of two turbulent parallel flow streams, and to compare the experimental values of the inner and outer jet boundaries with theoretical deductions.

B. Method

A ten percent mixture of hydrogen in air was injected co-axially into a three inch tube in which the velocity was 0.415 times that in the hydrogen mixture. At various points downstream from the point of mixing, traverses were made, and samples of mixture drawn off at intervals of 0.1 inch across the three inch tube. Hydrogen concentrations of each sample were measured by means of a calibrated thermo-conductivity cell. Velocities were measured by pitot tube.

C. Results

The principal results are shown as curves in Figures 8 to 24. These results are then compared to the only theoretical results available, those of Squire and

Transducer (3).

D. Conclusions and Recommendations

1) The method used in this investigation was accurate and rapid.

2) The thermo-conductivity cell offers an accurate means of measuring small concentrations of one gas in another where there is an appreciable difference between the thermal conductivities of the two gases.

3) For the conditions of this experiment, mixing was almost complete by the time the mixture had reached a distance of 61 diameters of the small tube from the point of mixing.

4) For sections near the point of mixing, and if wall effects are not present, velocity and concentration profiles are similar if plotted on a dimensionless basis.

5) For the conditions of this experiment, for $\lambda = 0.415$, the outer boundary of the mixing region is a straight line of slope 4^{o}-- $44'$.

6) Mixing along both outer and inner boundaries of the mixing region is extremely rapid until a distance of 22 diameters from the point of mixing is reached. From 22 diameters downstream, mixing is slower, and almost at a constant rate for all radii.

7) It is recommended that the experiment be repeated for various values of the velocity ratio, λ, and with turbulence promoters placed in the annulus of the outer pipe.

CHAPTER II

Introduction

Turbulent, or eddy diffusion, is the process of mixing by which mass transfer is effected in a turbulent fluid stream. Towle and Sherwood (2) have defined the eddy conductivity coefficient in a turbulent airstream at points greater than fifty diameters from the point of mixing. Little experimental work seems to have been undertaken, however, to determine the rate or method of mixing at points close to the mixing junction of two turbulent streams. Squire and Trouncer (3) have investigated, theoretically, the flow in a round jet issuing from an orifice in the same direction as a general external stream, and a comparison between their theoretical jet boundaries and the boundaries obtained experimentally by this work is given. The authors, also, attempted to determine the velocity and mass transfer profiles at various points near the point of mixing of two turbulent streams, and to compare these profiles in a qualitative and quantitative manner.

Oelheim and Thacher (1) demonstrated the practicality of using two thermo-conductivity cells to determine concentrations of hydrogen in air. This method seemed to be eminently feasible for use in quickly and easily finding

hydrogen concentrations at various points in fluid streams, and was adopted, therefore, for this use. It was necessary to set up and calibrate two thermo conductivity cells before the actual work of measuring rate of turbulent mixing could begin.

The testing procedure was as follows: A turbulent mixture of ten percent hydrogen in air was introduced co-axially through a one inch pipe into a three inch pipe. The three inch pipe contained pure air flowing at about one-half the velocity of the hydrogen-air mixture in the one inch pipe. At various distances from the point of mixture ranging from one-half the diameter of the small pipe to sixty-one times the diameter of the small pipe, hydrogen concentration and velocity traverses were made.

The authors believe an investigation of this type will be valuable in determining mixing lengths, jet boundaries of mixing regions, and mass transfer profiles for use in designing combustion chambers for rockets and gas turbines, or for any other mechanism where some knowledge of the relationship between velocity distribution and mass transfer profiles is necessary.

CHAPTER III

Description of Concentration Measuring Apparatus

Based on experimental work done in reference (1) it was initially decided to use the thermal conductivity cell as a method of measuring the volumetric concentration of one gas in a mixture with a second gas. A study of the thermal conductivity concentration factors for various gases showed that hydrogen had the greatest factor of advantage over air of any available gas, and since air had to be used as the reference gas, it was decided to use hydrogen as the mixing gas.

At 32°F. the thermal conductivity factor of hydrogen is .100 BTU/hr. (sq. ft.) (deg. F. per ft.) while that of air is .014. At 212°F, k. for hydrogen is .129 while .0183 for air. This gives a conductance factor of advantage to hydrogen over air varying from 7.15 at 32°F. to 7.05 at 212°F. By choosing a constant temperature of 82.5°F. at which to maintain the medium surrounding the cells this factor of advantage was maintained constant at a value of approximately 7.12 during the calibrations of the cell and the actual testing.

Two Leeds and Northrup thermal conductivity cells #Std.3284-F were used, one to hold a sample of air at room temperature (this cell to be hereafter referred to as

THEORETICAL CIRCUIT - CONCENTRATION MEASURING

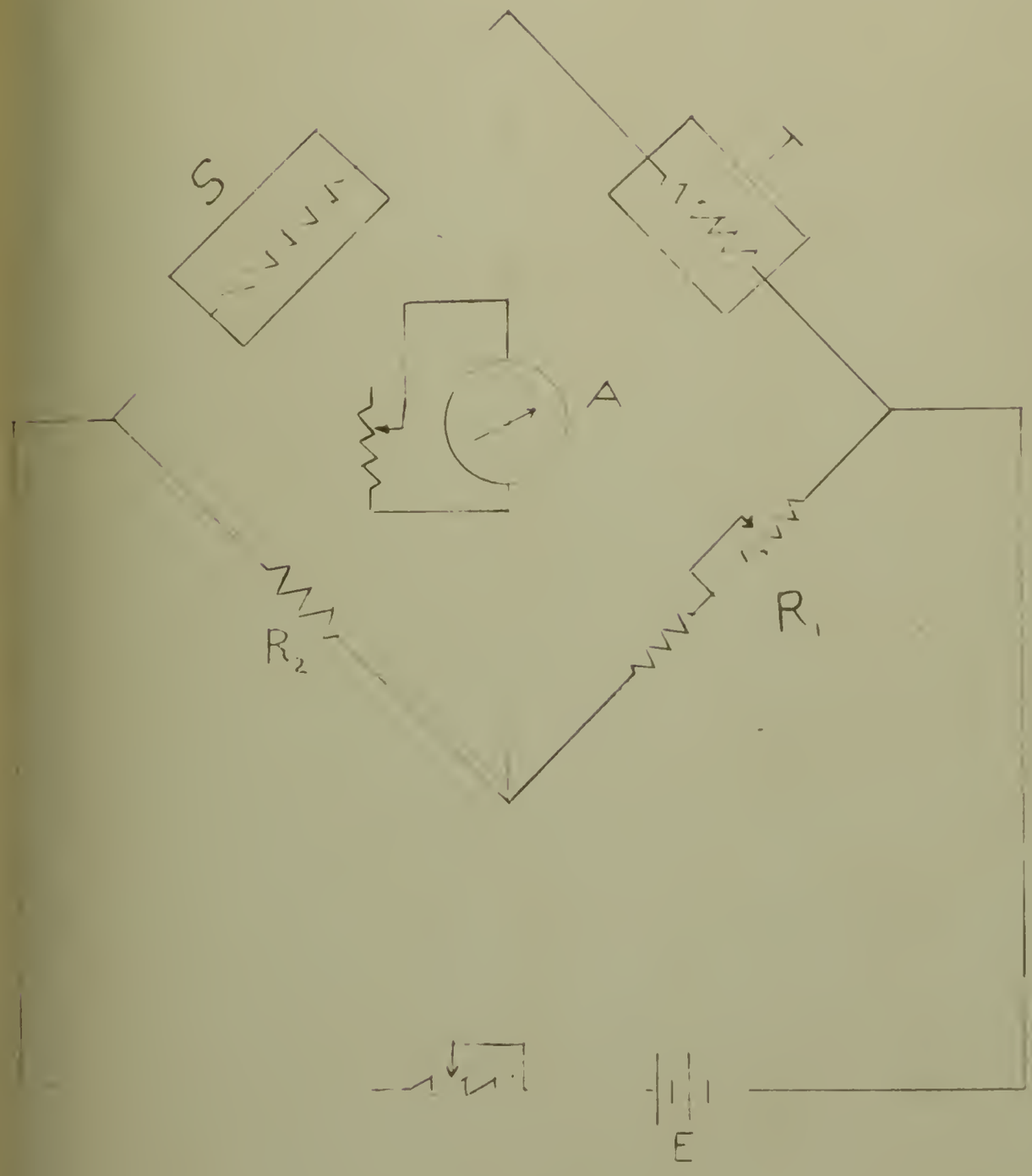

FIGURE 1

the standard cell) and the other to hold a sample of the gas mixture which was to be tested (hereafter referred to as the test cell). The standard and test cells formed the two arms of a Wheatstone bridge; the other two arms being (1) a resistance of 1000.9 ohms and (2) a variable decade box resistance in series with a variable 1 ohm maximum resistance. (See Figure 1.) A sample of room air was taken into the standard cell, and then a sample of the mixture into the test cell. By balancing the bridge, through which a current of 250 milliamperes is flowing, the apparent resistance of the test cell with respect to the standard cell can be obtained. Varying the percentage concentration of hydrogen in the test cell (the standard cell sample remaining constant) will cause this resistance ratio to vary, since the greater the hydrogen concentration in the test cell the greater the conductance of heat away from the wire in the cell, the less the temperature of this wire, and the less its resistance.

To start with, samples of room air were taken into both cells; and the resistance of the variable arm of the bridge was measured by balancing the bridge. This resistance value was used as a reference. Next, known volumetric concentrations of hydrogen in air were put successively in the test cell, the original sample of room air remaining in the standard cell. A plot of the resistance reading

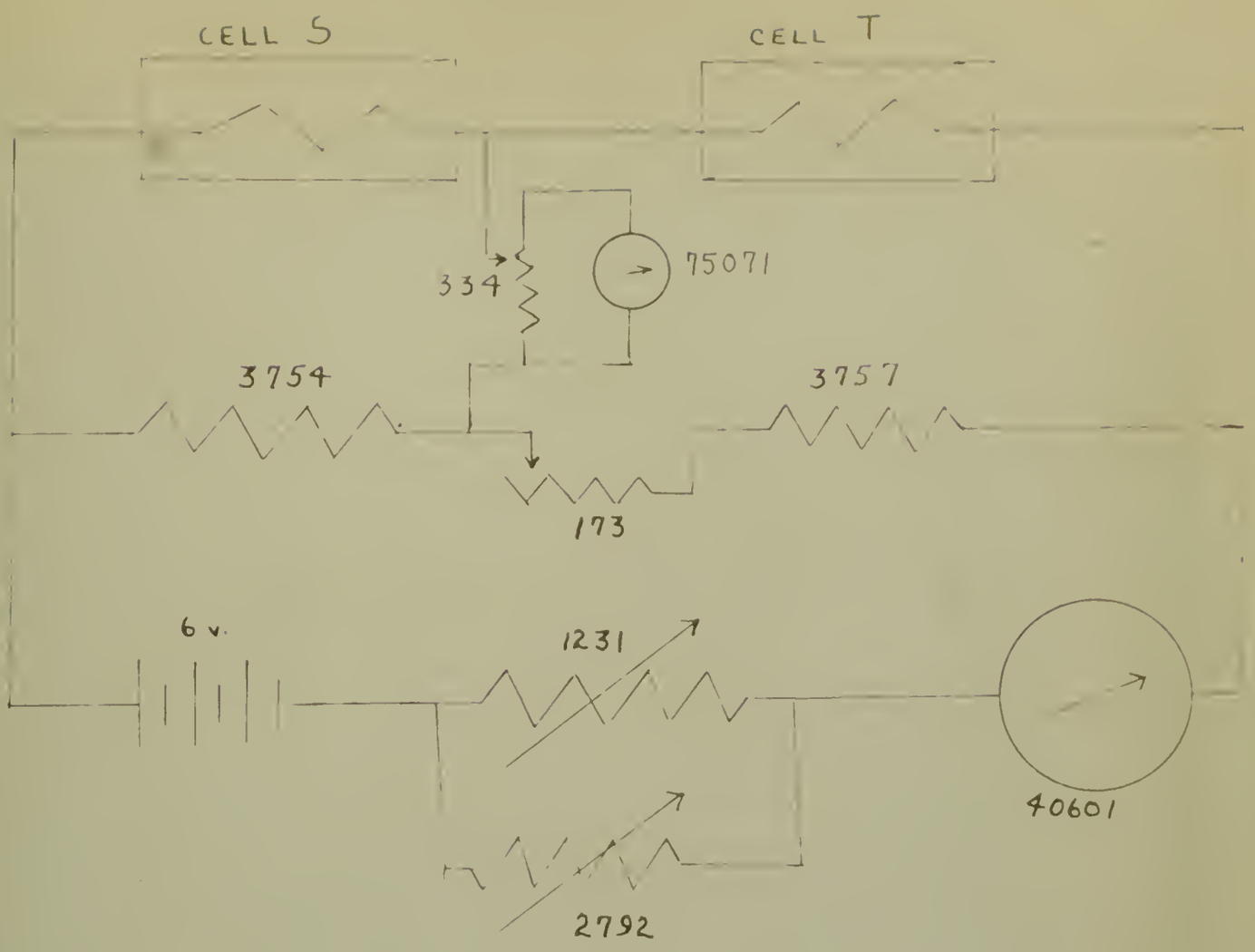

ACTUAL CIRCUIT

3757	HARTMAN AND BRAUN	10,000 Ω DECADE
173	GENERAL RADIO	1 Ω DECADE
334	AYRTON	10,000 Ω SHUNT
75071	LEEDS & NORTHRUP	4×10^{-8} AMP/M.M GALVANO
3754	HARTMAN AND BRAUN	10,000 Ω DECADE
2792		7.5 Ω SLIDEWIRE
1231	OHMITE	12 Ω SLIDE WIRE
40601	COMM'L.	0.750 AMP D.C. AMMETER

ALL NUMBERS EXCEPT 40601 REFER TO L.F. DEPT. M.I.T.

FIGURE 2

for each sample minus the reference reading vs. percentage concentration of hydrogen was made. This calibration plot was later used to measure the hydrogen concentration across the traverse in the eddy mixing apparatus.

Figure 2 is a diagramatic sketch of the entire concentration measuring apparatus. As is seen, a battery source was used to provide 250 milliamps. This current was maintained constant by varying the paralleled variable resistors 2792 and 1231. By the use of the 750 milliameter #40601 the current could be set to within 0.5 milliamps of the desired value. Resistor #3754 was set at a measured value of 1000.9 ohms, and resistor #3757 in series with a 0.1 ohm step variable resistor #173 was used to balance the bridge. A 4×10^{-8} amp/mm. Galvanometer, paralleled by an Aryton shunt would permit resistance readings to 0.01 ohm but it was never deemed necessary to measure resistances closer than to 0.1 ohm since this resistance would detect a 0.01% hydrogen concentration in air. Closer work than this was not necessary.

The two thermal conductivity cells were immersed in a constant temperature water bath which was maintained within 0.2°C of the datum used (28.0°C). Varying of the water temperature through 0.2° C did not seem to change the resistance readings within the 0.1 ohm allowable. A heating element was used to maintain the bath temperature, and a motor driven stirrer kept the water circulating past

the cells. The motor was stopped just before taking a reading as it was felt that the natural water circulation would be more uniform around the cells than induced circulation.

The gas sample to be measured was sucked into the test cell and the cell closed during a reading. No flow in the side tube was permitted during this time. Before a new sample was brought into the test cell the old sample was evacuated with a vacuum pump which could maintain less than 1" Hg. Since two suctions were always taken in an evacuation (suction on the old sample, cell filled with new sample, suction on new sample, cell again refilled with new sample) the effect of the remaining portion of the old sample in the cell would be negligible. 1/900 part of the old sample is all that could remain. Since we were operating with concentrations of 10% and less of hydrogen in air, the maximum error would be about 0.01% hydrogen or 0.1 ohm resistance reading. This was considered allowable.

CHAPTER IV

Calibration of Thermal Conductivity Cell Apparatus

The calibration of the thermal conductivity cell apparatus to plot a curve of hydrogen volumetric concentration in the gas mixture versus variable resistance reading on the arm of the Wheatstone bridge was conducted as follows in a constant temperature room:

1. Glass tubing and bulbs were set up as shown in Figure 3.

2. Bulbs I, II, and III and all connecting tubing were filled with Hg. by raising the level of the three mercury containers.

3. A flexible connection was made to a hydrogen bottle through a differential valve which would lower the gas pressure from 2300 psi to a few lbs. gage. Hydrogen was then blown through the connection to blow out any trapped air.

4. The flexible connection was attached to port #1 of valve "A." Valves "A," "B," and "C" were set to provide a clear passage from port #1 to port #8 and hydrogen was blown through this passage to clear out any air which might have remained trapped in the connections.

5. Valve "A" set so that hydrogen flowed into port #3 under a slight pressure which was maintained by keeping

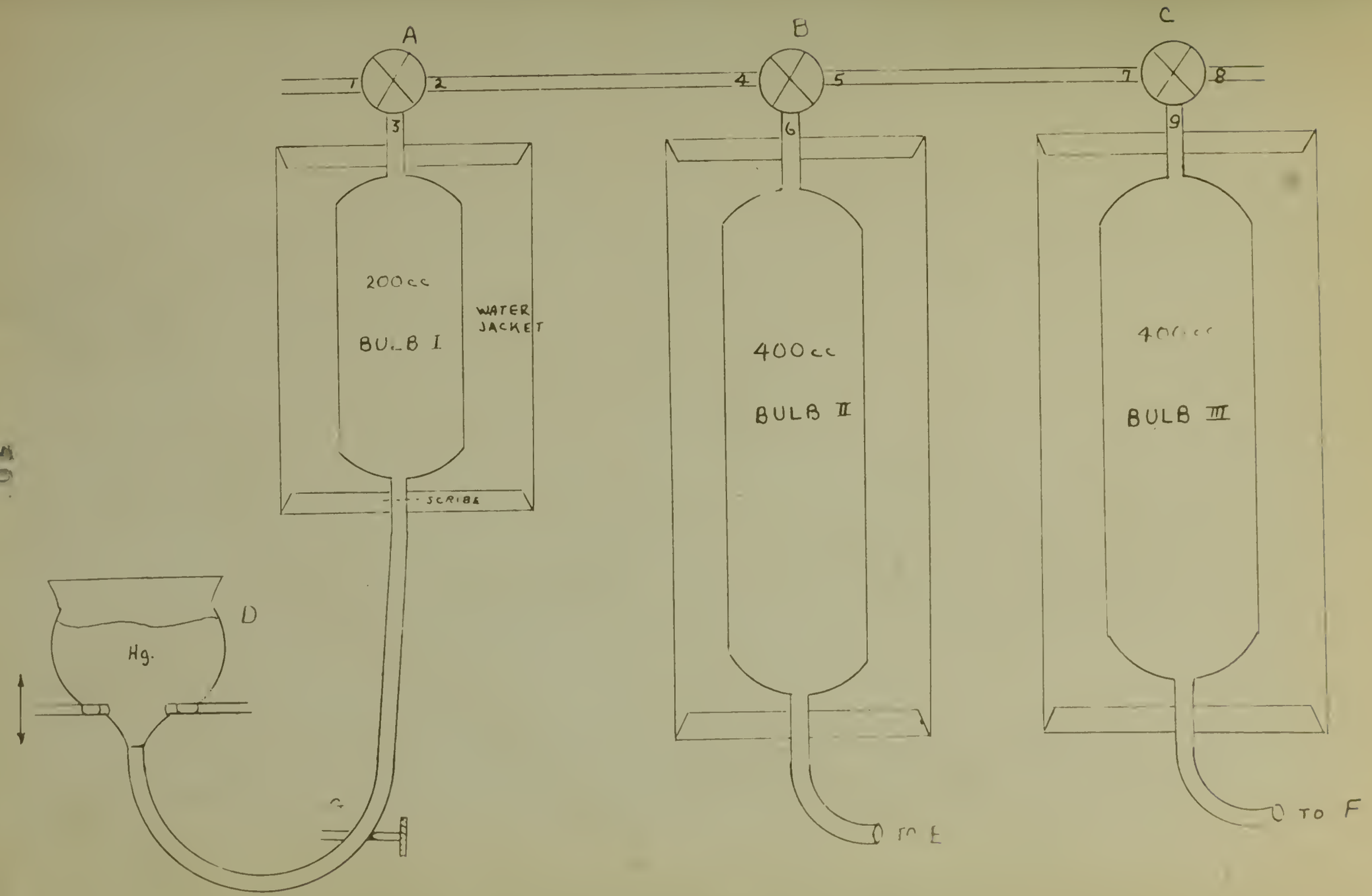

CALIBRATION APPARATUS

FIGURE 3

the level of Hg. in "D" above that in "I." The Hg. in "I" was pushed down to a scribe mark in the capillary tubing as shown in the sketch. Stop "G" and valve "A" were closed and the hydrogen allowed to sit in bulb "I" until temperature equilibrium was reached with the cooling water in the jacket surrounding the bulb.

6. The hydrogen connection was disconnected from valve "A."

7. Atmospheric pressure was obtained in bulb "I" by opening valve "A" to atmosphere and allowing hydrogen to escape until pressure equilibrium reached.

8. Valves "A" and "B" are set so that passage between ports #3 and #6 results. By manipulating the heights of the Hg. in bulbs "D" and "E" the hydrogen sample was pushed into bulb "II," displacing the Hg.

9. Valve "B" closed and a sample of room air taken into bulb "I" through valve "A" by lowering level of bulb "D" until air reached scribe mark. Valve "G" closed and the air sample allowed to reach temperature equilibrium with the jacket water.

10. Air sample next pushed into bulb "II" by procedure as in step 8.

11. Air and hydrogen samples mixed thoroughly by passing the mixture from bulb "II" to bulb "III" and back for three cycles. Finally, a 50% hydrogen-air mixture was obtained in bulb "III" ready for sampling.

12. Samples of room air were drawn into the standard and test thermal conductivity cells and a "zero reading obtained of the variable resistance arm of the Wheatstone bridge. The air sample from the test cell was completely evacuated and a sample of the 50% concentration pushed into the test cell for a reading. Two such samples could be obtained for each percentage concentration.

13. Half of the above 50% sample was then pushed back into bulb "I" and the rest of the apparatus filled with mercury. Step 8 was repeated with this sample. Step 9 repeated with a new air sample. Steps 10 and 11 repeated with the resultant 25% sample finally available in bulb "III." Half of this sample was again used for tests in the cells.

14. By similar procedure, test samples were made available in concentrations varying from 50% hydrogen-air to 0.01% hydrogen-air.

CHAPTER V

Results of Thermal Conductivity Cell Calibration

By using the method of obtaining known hydrogen-air concentration samples as outlined in Chapter IV and by using these samples in the thermal conductivity test cell with an air sample in the standard cell, it was possible to obtain resistance readings of the variable arm of the Wheatstone bridge. The resistance reading obtained thusly was subtracted from the "zero reading" of the concentration measuring apparatus when air samples were placed in both cells, and this delta R reading was plotted against the percentage hydrogen-air concentration. Four calibration runs were made and plotted, (data and graphs included as sheet "I" and graph Figures 4,5,6.) The average error of resistance readings between runs of the same concentration was 0.24 ohms, which is approximately 0.03% hydrogen. Since a mixture of 10.0% hydrogen was used in the central stream of the mixing apparatus, this possible error in the calibration would not be too excessive. The sensitivity of the cell in detecting, although not be able to consistently and accurately measure, a 0.01% hydrogen concentration gives promise of using this devise for more accurate work than was considered necessary here.

Several factors were noticed which influenced the bridge resistance readings, and these factors were minimized

as stated below.

(a) Bath temperature affected "zero reading." This was minimized by maintaining the bath constant within .2°C.

(b) Varying the inclination of the cells affected "zero." Cells were clamped in place.

(c) Varying height of water bath and agitation of water varied zero. Water bath height maintained constant. Water stirred mechanically until about a half minute before reading when the stirrer was stopped and the water allowed to flow past the cells by natural inertia of flow.

(d) Any portion of an old sample that remained in the test cell would affect the reading of the new sample. This was minimized by taking a double suction on the old sample (old sample evacuated, new sample drawn in and evacuated before a reading taken.) This factor may have been responsible for part of the error as mentioned in the above discussion.

(e) Impurity of the original hydrogen. This was stated by the supplier to be less than .01%.

(f) Incorrect measurement of air and hydrogen samples in 200 cc bulb "I" of Figure 3. This was nullified by using the scribe mark in the capillary tubing as the reference for measuring the volume of each of the constituent gases.

(g) Impurities of CO_2 and H_2 in the air. Since samples of the same air were used in both cells for the

"zero reading" this will practically nullify any error which might result from normal changes in the impurities in the air from day to day. (The hydrogen concentration, delta R plot is of almost constant slope throughout its lower region.)

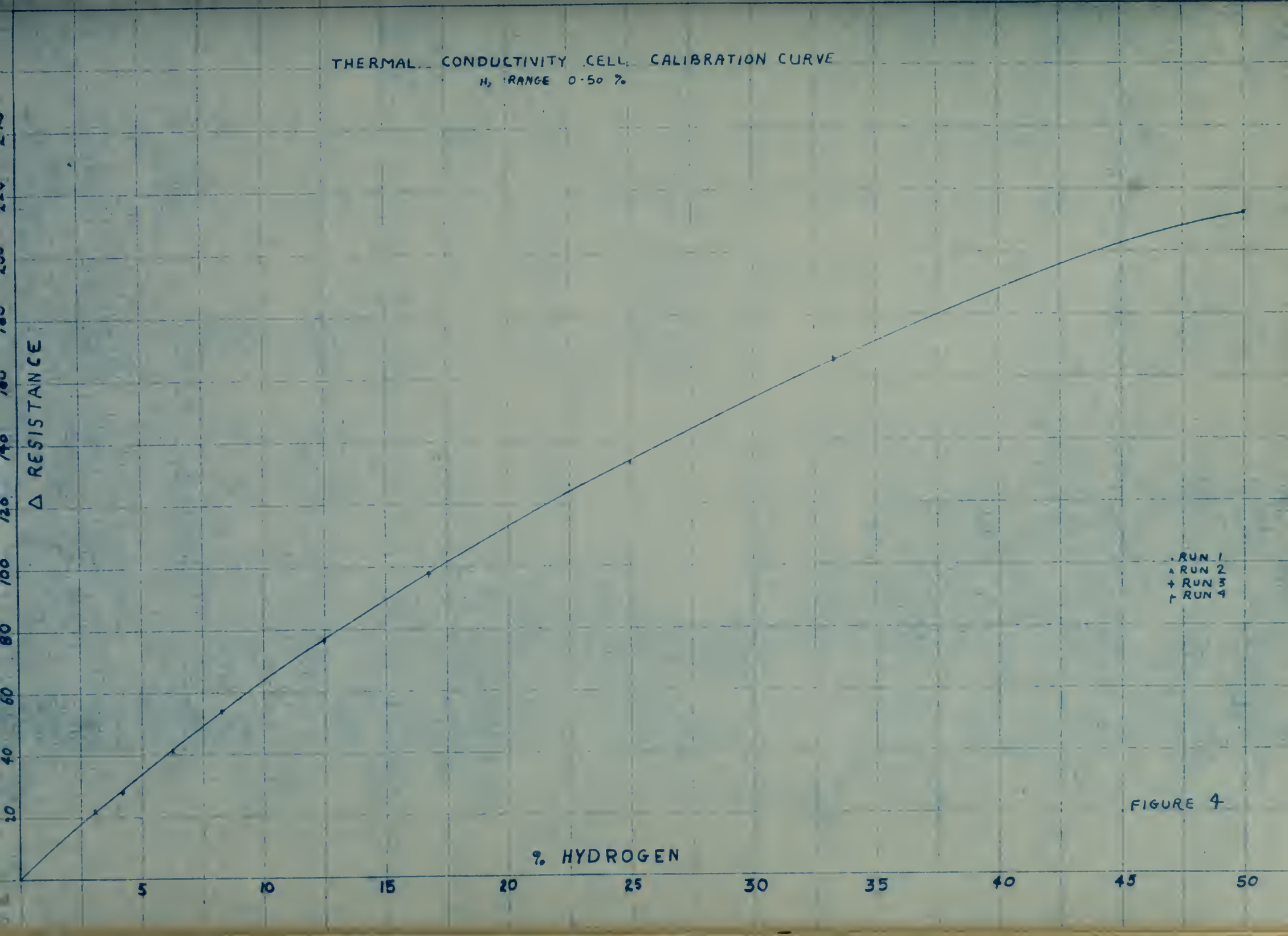
THERMAL CONDUCTIVITY CELL CALIBRATION CURVE
H2 RANGE 0-50 %
Δ RESISTANCE
% HYDROGEN
RUN 1
RUN 2
RUN 3
RUN 4
20
40
60
80
100
120
140
5
10
15
20
25
30
35
40
45
50

FIGURE 4

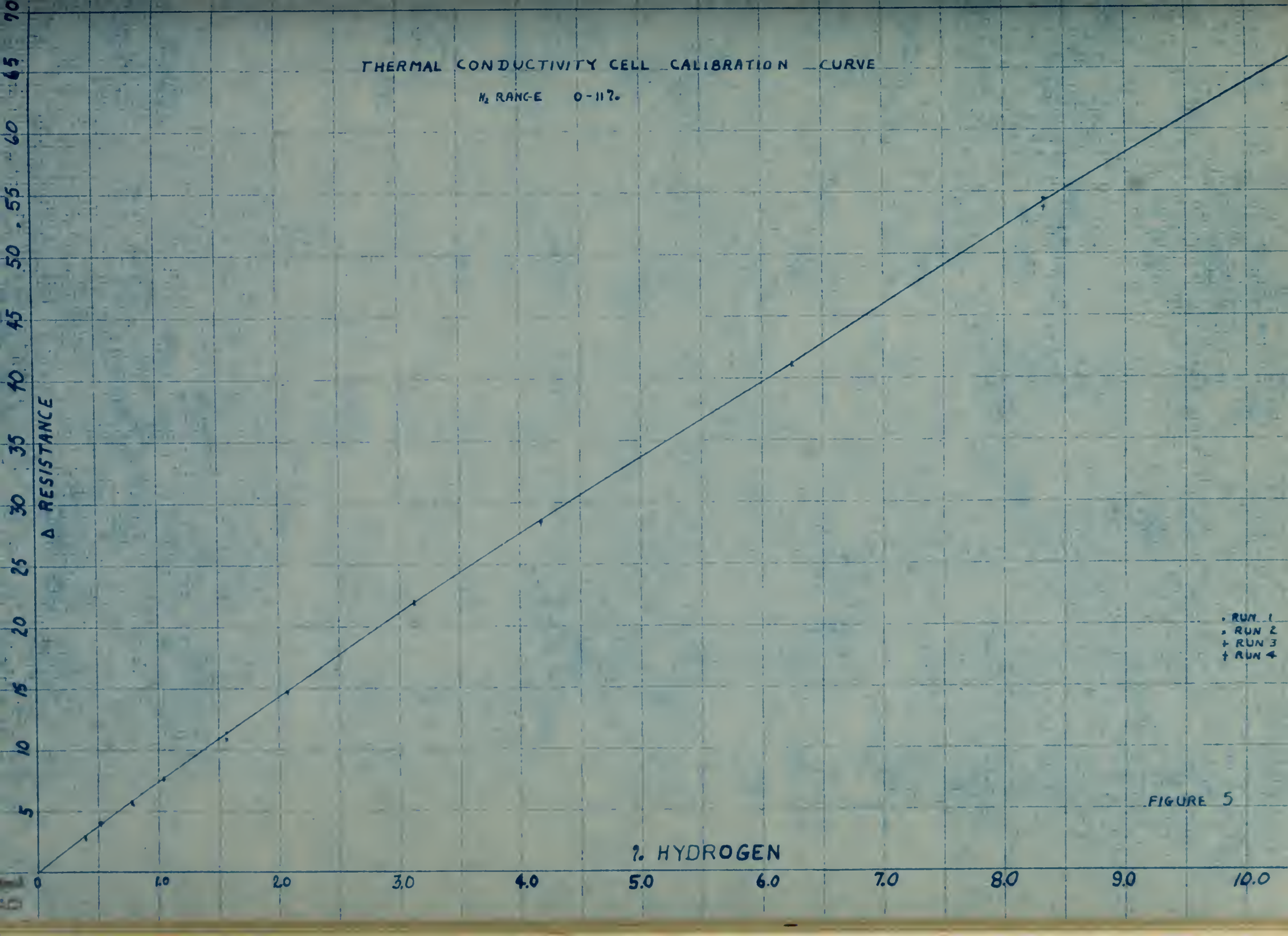
THERMAL CONDUCTIVITY CELL CALIBRATION CURVE
H_2 RANGE 0-11%
Δ RESISTANCE
% HYDROGEN
0
1.0
2.0
3.0
4.0
5.0
6.0
7.0
8.0
9.0
10.0
5
10
15
20
25
30
35
40
45
50
55
60
65
70
• RUN 1
▪ RUN 2
+ RUN 3
+ RUN 4

FIGURE 5

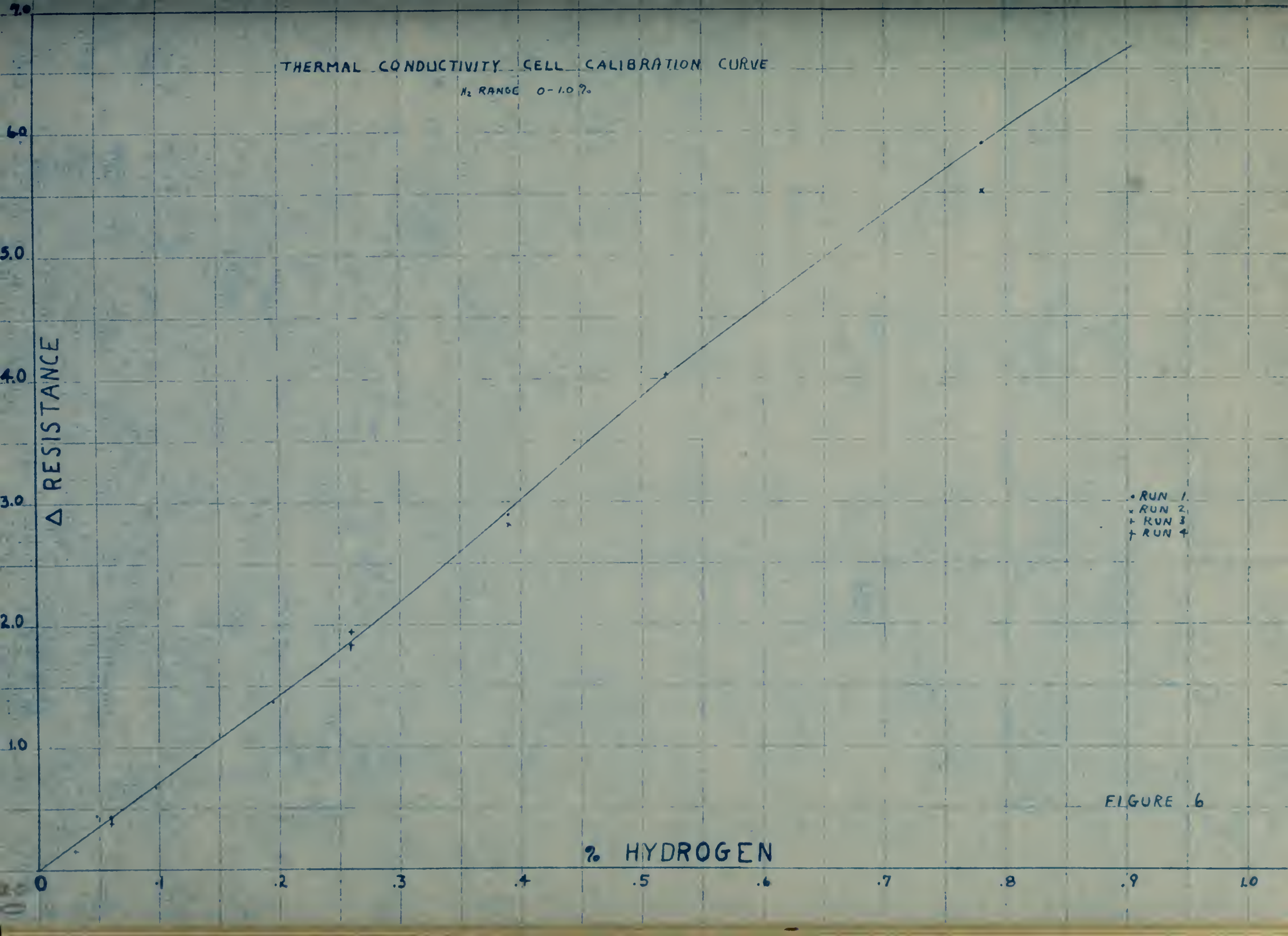
THERMAL CONDUCTIVITY CELL CALIBRATION CURVE
H_2 RANGE 0-1.0 %
Δ RESISTANCE
% HYDROGEN
7.0
6.0
5.0
4.0
3.0
2.0
1.0
0
.1
.2
.3
.4
.5
.6
.7
.8
.9
1.0
• RUN 1
× RUN 2
+ RUN 3
† RUN 4

FIGURE .6

CHAPTER VI

Description of Apparatus and Procedure

The apparatus for conduction of the test runs of this thesis is shown in Figure 7. A three inch brass pipe, 180 inches in length is so arranged that a suction can be taken on it by the Spencer turbine. It is equipped with taps at various stations along its length where a micrometer traversing mechanism may be screwed into it. When the traversing mechanism is not inserted in a tap hole, a brass plug, machined to fit the inner contour of the three inch pipe, is inserted. At the end of the three inch pipe nearest the Spencer turbine a sharp edged orifice meter is fitted in order to measure total flow. At its open end the three inch pipe is fitted with a forged bellmouth in order to allow the air stream to enter with the least possible resistance.

A one inch pipe is inserted axially and concentrically with the three inch pipe at the latter's belled end. The one inch pipe is centered in the three inch by means of a bakelite centering piece, leveled by spirit level to put both pipes in the same horizontal plane, and placed in the same vertical plane by a plumb bob arrangement. Vertical alignment is checked by a velocity traverse to determine that the upper and lower velocity profiles are symmetrical. The end of the one inch pipe is tapered to

a sharp point so that there will be as little interference, due to wall thickness, as possible at the juncture of the two streams. A Chicago air compressor supplying a bank of receivers furnishes the air for the one inch pipe. The mass flow from the receivers to the one inch pipe is regulated by maintaining a constant predetermined pressure above a rounded entrance orifice by means of a bleed off valve on the receiver line. Hydrogen is introduced through a constant pressure valve on a manifold connecting six standard hydrogen bottles simultaneously. It is metered through a thin plate sharp edged orifice and introduced into the one inch line twenty feet and two ninety degree angles from the mixing point.

The traversing mechanism is a No. 18 hypodermic needle cut to a length of 1 3/16 inches and mounted at right angles to a 1/8 inch copper tube. The copper tubing is mounted in a micrometer which may be screwed into any of the tap holes. By this means the hypodermic sampling needle's position can be established within .001 inch in the three inch tube.

To make a traversing run, the Chicago air compressor was started, the Spencer turbine started, and flow in the two pipes adjusted until the maximum velocity in the one inch pipe was 176 ft/sec and the maximum velocity in the three inch annulus was 74 ft/sec. These velocities are equivalent to Reynolds numbers of 79,100 in the one inch

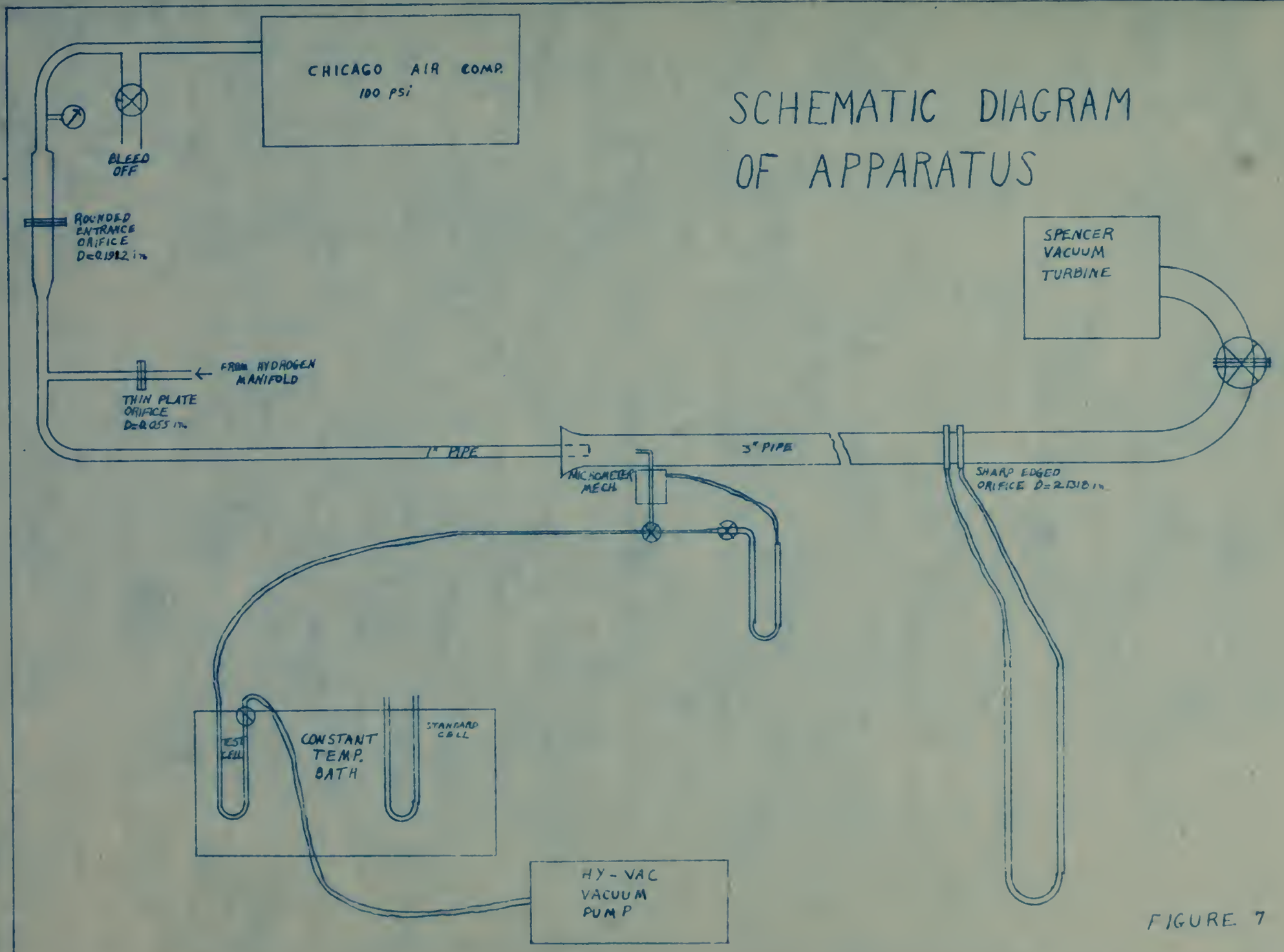
SCHEMATIC DIAGRAM OF APPARATUS
CHICAGO AIR COMP. 100 PSI
BLEED OFF
ROUNDED ENTRANCE ORIFICE D=0.1912 in.
FROM HYDROGEN MANIFOLD
THIN PLATE ORIFICE D=0.055 in.
1" PIPE
3" PIPE
MICROMETER MECH.
SPENCER VACUUM TURBINE
SHARP EDGED ORIFICE D=2.018 in.
TEST CELL
CONSTANT TEMP. BATH
STANDARD CELL
HY-VAC VACUUM PUMP

FIGURE 7

pipe and 107,000 in the three inch at the point of mixing.

Hydrogen was introduced into the one inch pipe until a concentration of about ten percent was obtained. With the traversing mechanism inserted in the hole in question and connected so that the hypodermic needle was pointing directly upstream, a high vacuum was produced in the thermo conductivity test cell and in the tubing connecting it to the hypodermic needle. When a sufficiently high vacuum had been reached, the valve connecting the hypodermic needle to the test cell was opened and a sample taken into the test cell. A sample of room air similar to that supplied to the bellmouth of the three inch pipe was introduced into the standard thermo conductivity cell and a resistance reading for balance in the Wheatstone bridge was taken. Usually this procedure was repeated several times at each point in the traverse to obviate any errors due to residue gases from the previous sample remaining in the test cell.

After the hydrogen concentration had been obtained in this manner, the velocity head at the point in question was found by connecting the hypodermic needle to a manometer, the other side of which was connected to a standard pressure tap in the base of the micrometer mechanism within the tube.

Traverses were thus made across a diameter of the three inch pipe taking readings at each 0.1 inch.

Hydrogen content of the one inch gas stream was maintained constant by taking several samples from the one

inch pipe at various times during the traversing run. At all times the variation of hydrogen in the one inch stream was well within the limits of accuracy of the experiment.

CHAPTER VII

Results

Table III shows the numerical results of a representative traverse. Table II indicates the distance from the mixing point to the various traverses. All other results are presented in the form of curves shown in Figures 8 to 24.

Figures 8 and 9 are indications of hydrogen concentrations in percent versus diameter at traverses in holes A through L. Figures 10, 11 and 12 show velocity profiles of point velocities versus diameters for the same traverses as above. Figures 13 through 21 are plots of velocity and concentration profiles on a dimensionless basis where the ratio $\frac{C}{C_1}$ is the ratio of concentration at the point in question to the maximum concentration at that traverse and $\frac{V-V_2}{V_1-V_2}$ is the velocity at any point minus the base velocity for the three inch pipe divided by the maximum velocity for the traverse in question minus the base velocity. These velocities are shown in the accompanying sketch 7b. Wherever base velocity was indeterminable, it was assumed to be 74 ft/sec.

Figure 22 is a series of contour curves of constant hydrogen concentration obtained by drawing cross curves from Figures 8 and 9. For example, all points between the

5 and 6 percent curves will have a hydrogen content of less than 6 percent, but greater than 5 percent.

Figure 23 is a plot of hydrogen concentrations versus distance from mixing point for constant radii. By extrapolating these curves, it was possible to obtain data for Figure 24, which outlines the boundaries of the jet where the hydrogen is a maximum and the hydrogen is zero. That is, $\frac{r_o}{a}$ and $\frac{r_i}{a}$ vs. $\frac{x}{a}$. The resulting curves are compared to the theoretical values obtained from the analysis of Squire and Trouncer (3).

DIAGRAM ILLUSTRATING NOTATION

FIGURE 7b

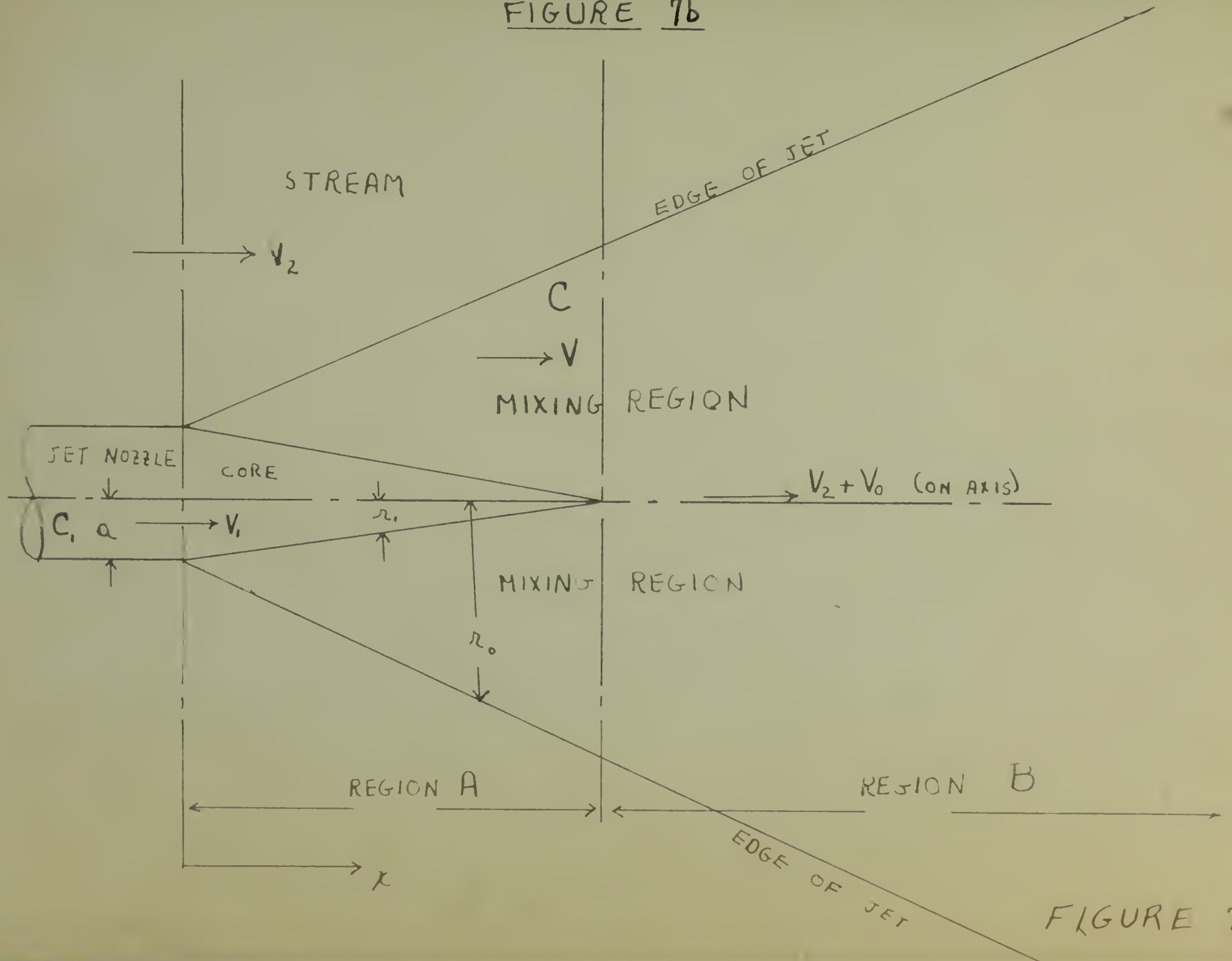

FIGURE 7b

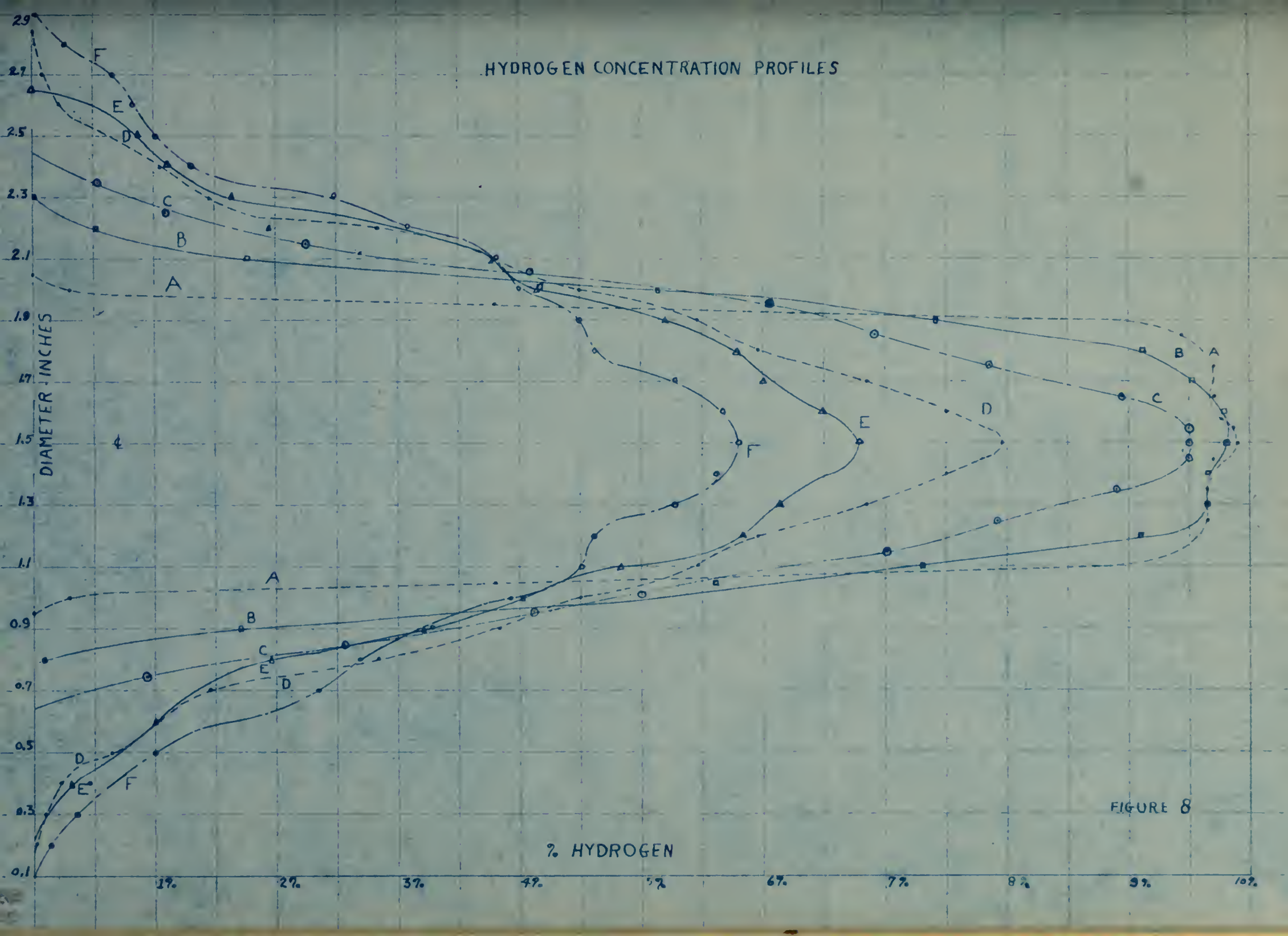
HYDROGEN CONCENTRATION PROFILES
DIAMETER INCHES
% HYDROGEN
2.9
2.7
2.5
2.3
2.1
1.9
1.7
1.5
1.3
1.1
0.9
0.7
0.5
0.3
0.1
1%
2%
3%
4%
5%
6%
7%
8%
9%
10%
A
B
C
D
E
F

FIGURE 8

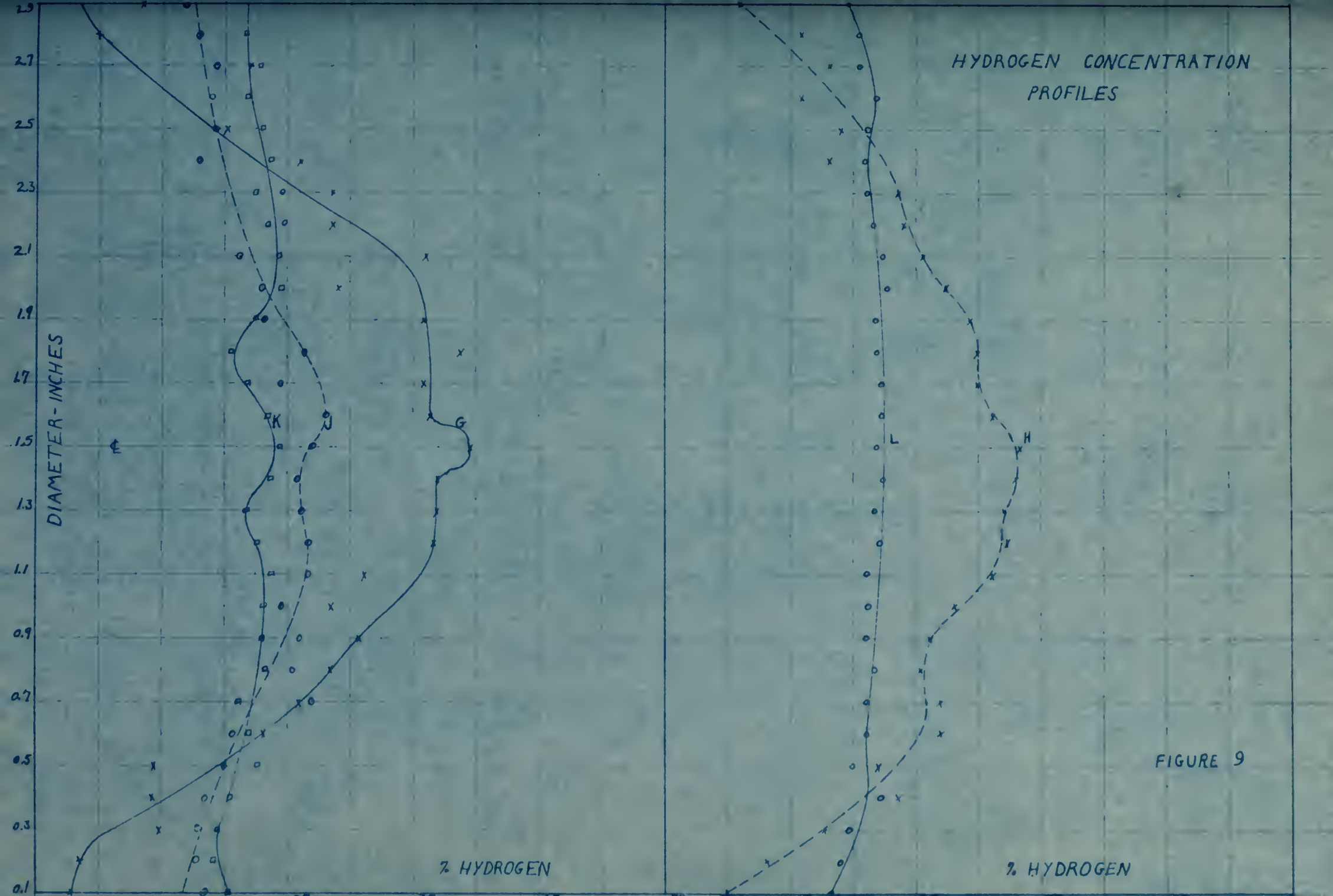
HYDROGEN CONCENTRATION PROFILES
DIAMETER - INCHES
2.9
2.7
2.5
2.3
2.1
1.9
1.7
1.5
1.3
1.1
0.9
0.7
0.5
0.3
0.1
K
J
G
L
H
% HYDROGEN
1%
2%
3%
4%
5%
% HYDROGEN
1%
2%
3%
4%
5%

FIGURE 9

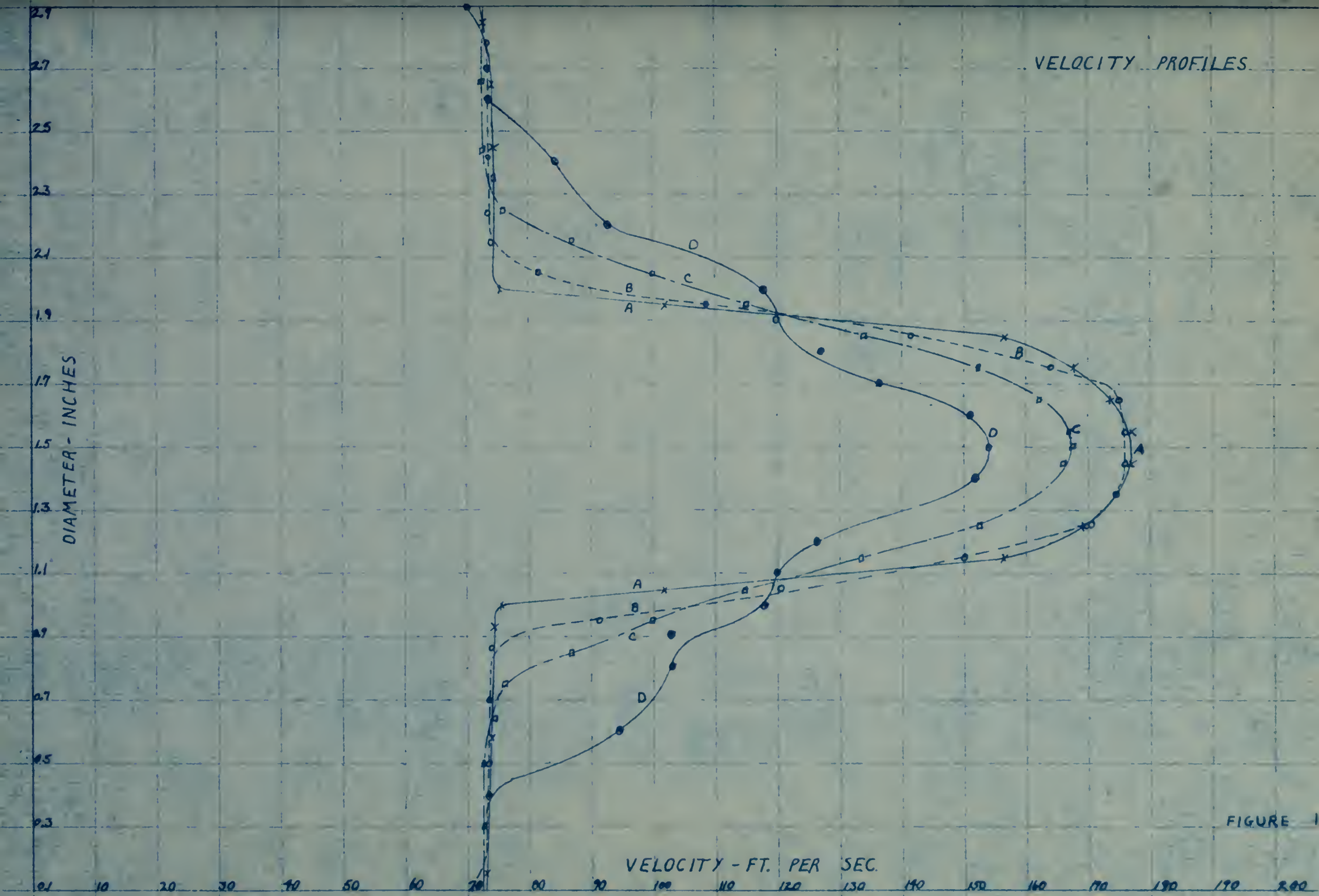
VELOCITY PROFILES
DIAMETER - INCHES
2.9
2.7
2.5
2.3
2.1
1.9
1.7
1.5
1.3
1.1
0.9
0.7
0.5
0.3
A
B
C
D
VELOCITY - FT. PER SEC.
0.1
10
20
30
40
50
60
70
80
90
100
110
120
130
140
150
160
170
180
190
200

FIGURE 1

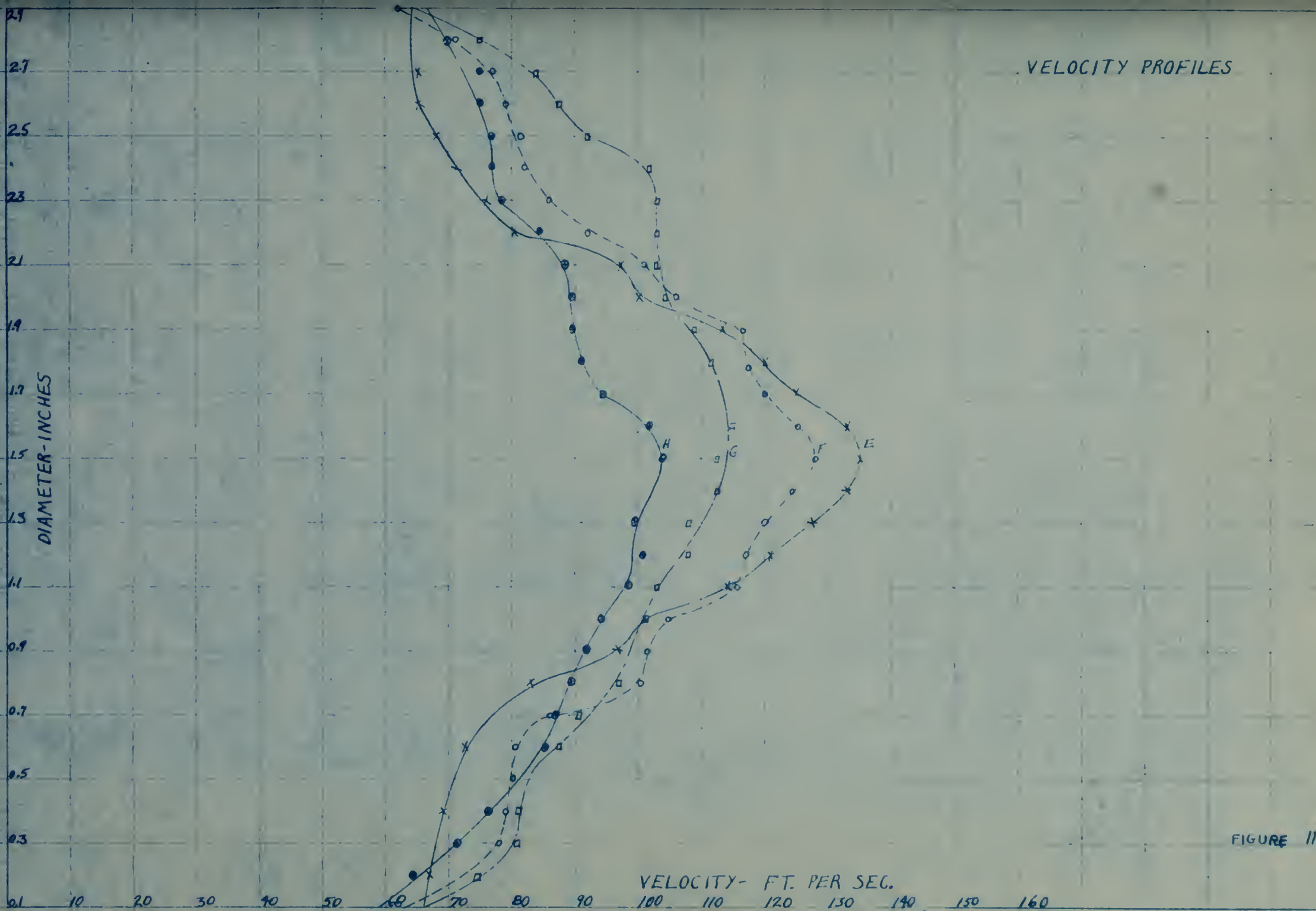
VELOCITY PROFILES
DIAMETER-INCHES
2.9
2.7
2.5
2.3
2.1
1.9
1.7
1.5
1.3
1.1
0.9
0.7
0.5
0.3
0.1
H
G
F
E
10
20
30
40
50
60
70
80
90
100
110
120
130
140
150
160
VELOCITY- FT. PER SEC.

FIGURE 11

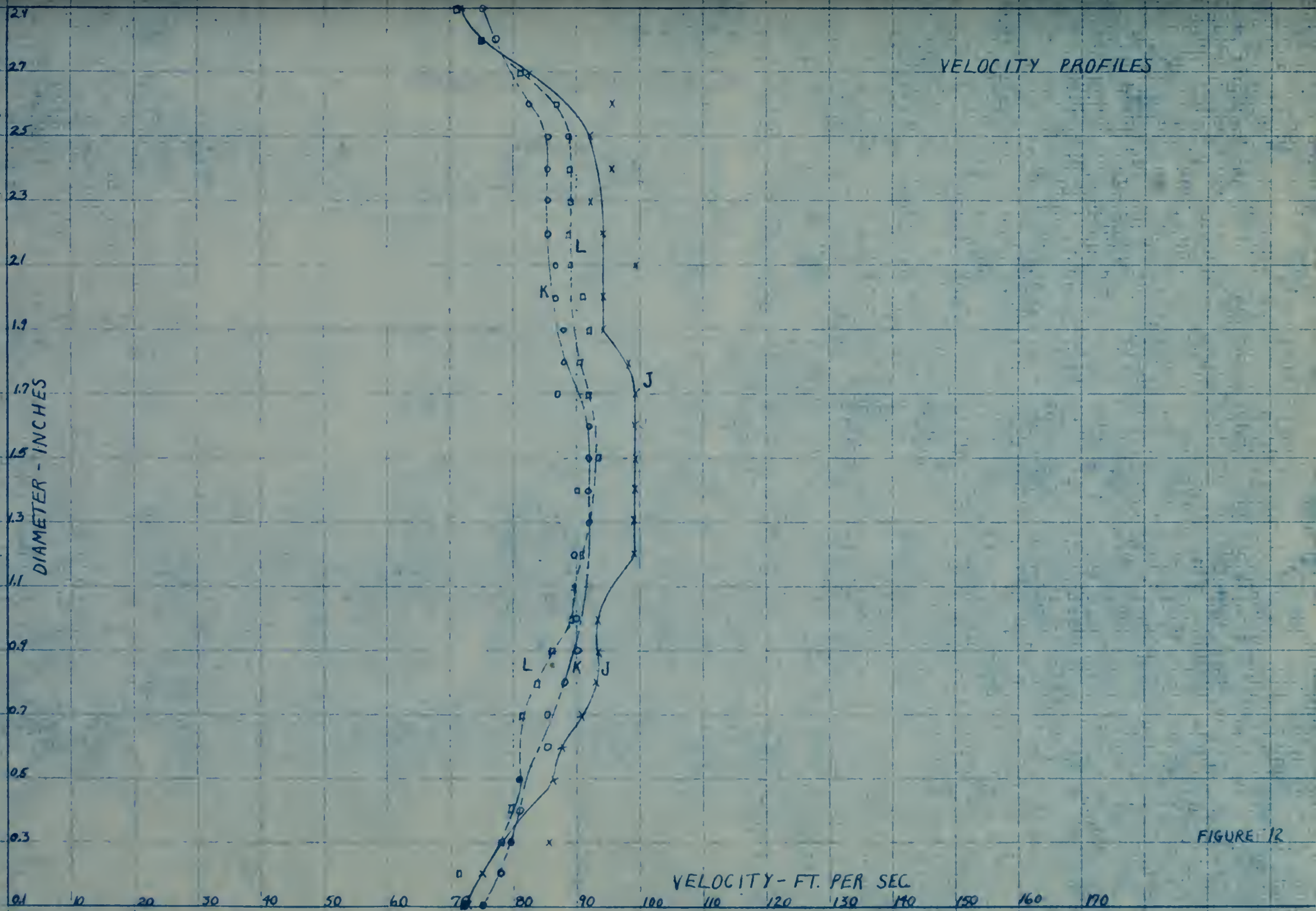
VELOCITY PROFILES
DIAMETER - INCHES
2.9
2.7
2.5
2.3
2.1
1.9
1.7
1.5
1.3
1.1
0.9
0.7
0.5
0.3
0.1
L
K
J
L
K
J
10
20
30
40
50
60
70
80
90
100
110
120
130
140
150
160
170
VELOCITY - FT. PER SEC.

FIGURE 12

PROFILE COMPARISON HOLE "A"

FIGURE 13

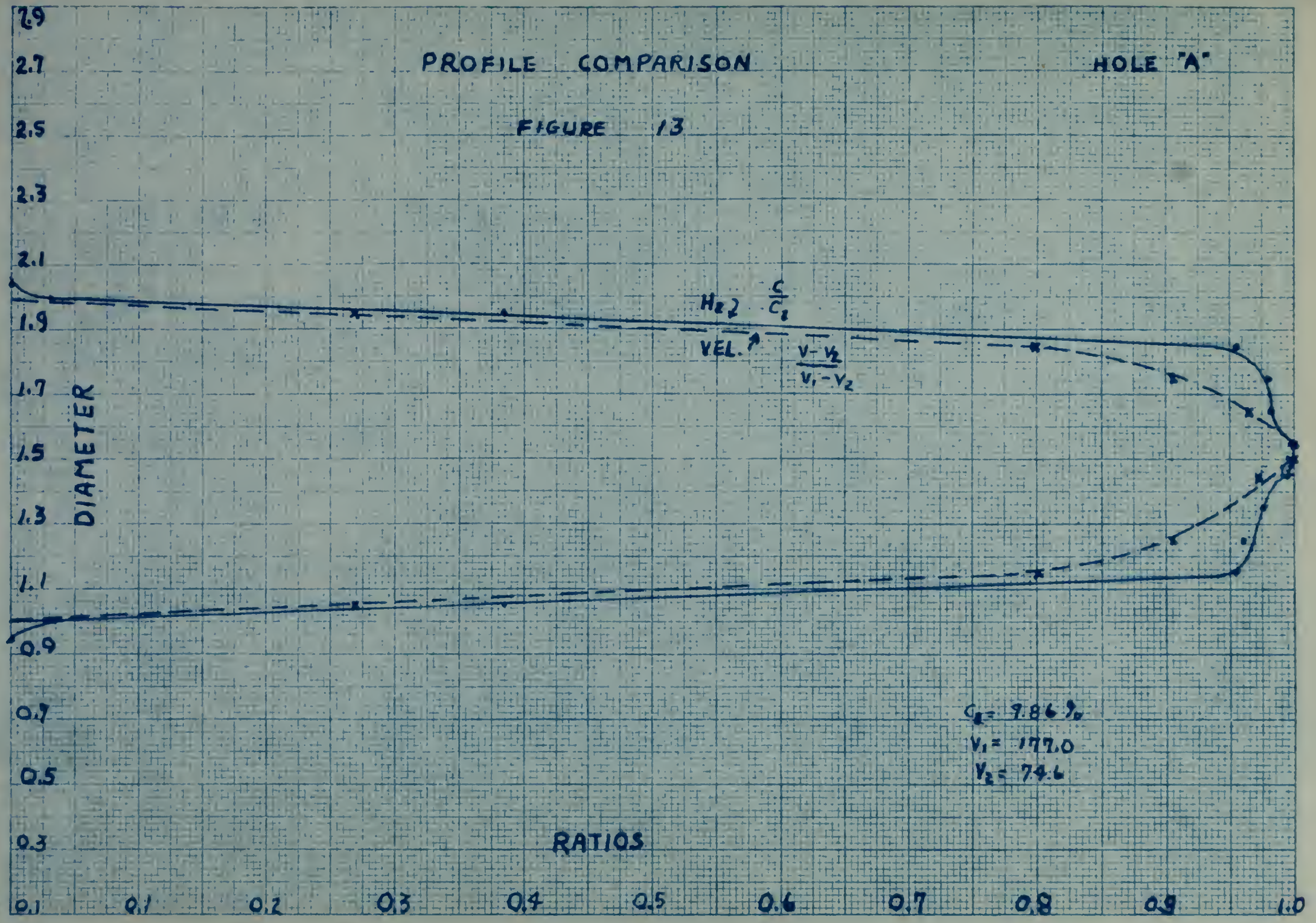

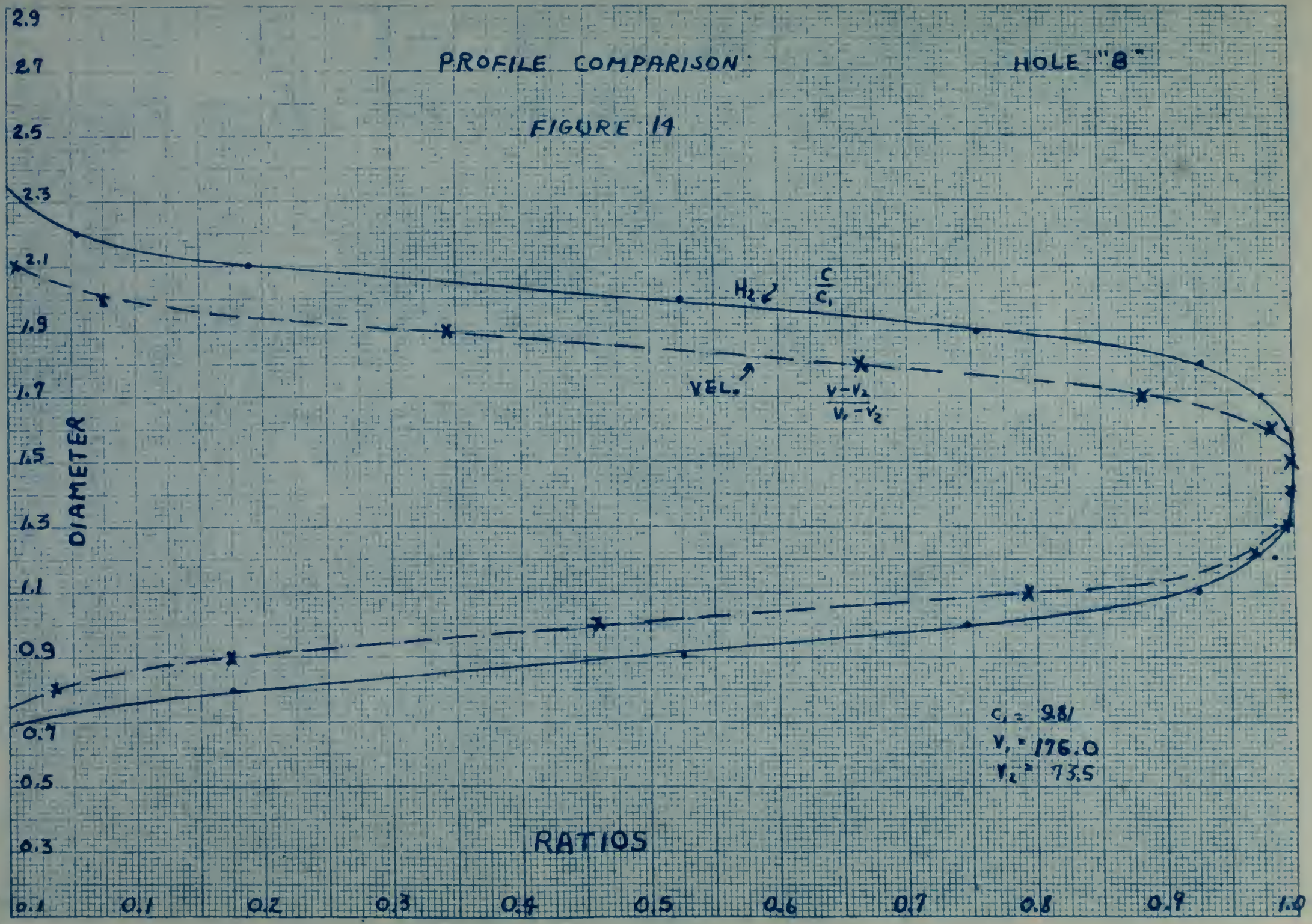
PROFILE COMPARISON
HOLE "B"
FIGURE 14
DIAMETER
RATIOS
H_2
$\frac{C}{C_1}$
VEL.
$\frac{V-V_2}{V_1-V_2}$
$C_1 = 9.81$
$V_1 = 176.0$
$V_2 = 73.5$
2.9
2.7
2.5
2.3
2.1
1.9
1.7
1.5
1.3
1.1
0.9
0.7
0.5
0.3
0.1
0.2
0.3
0.4
0.5
0.6
0.7
0.8
0.9
1.0

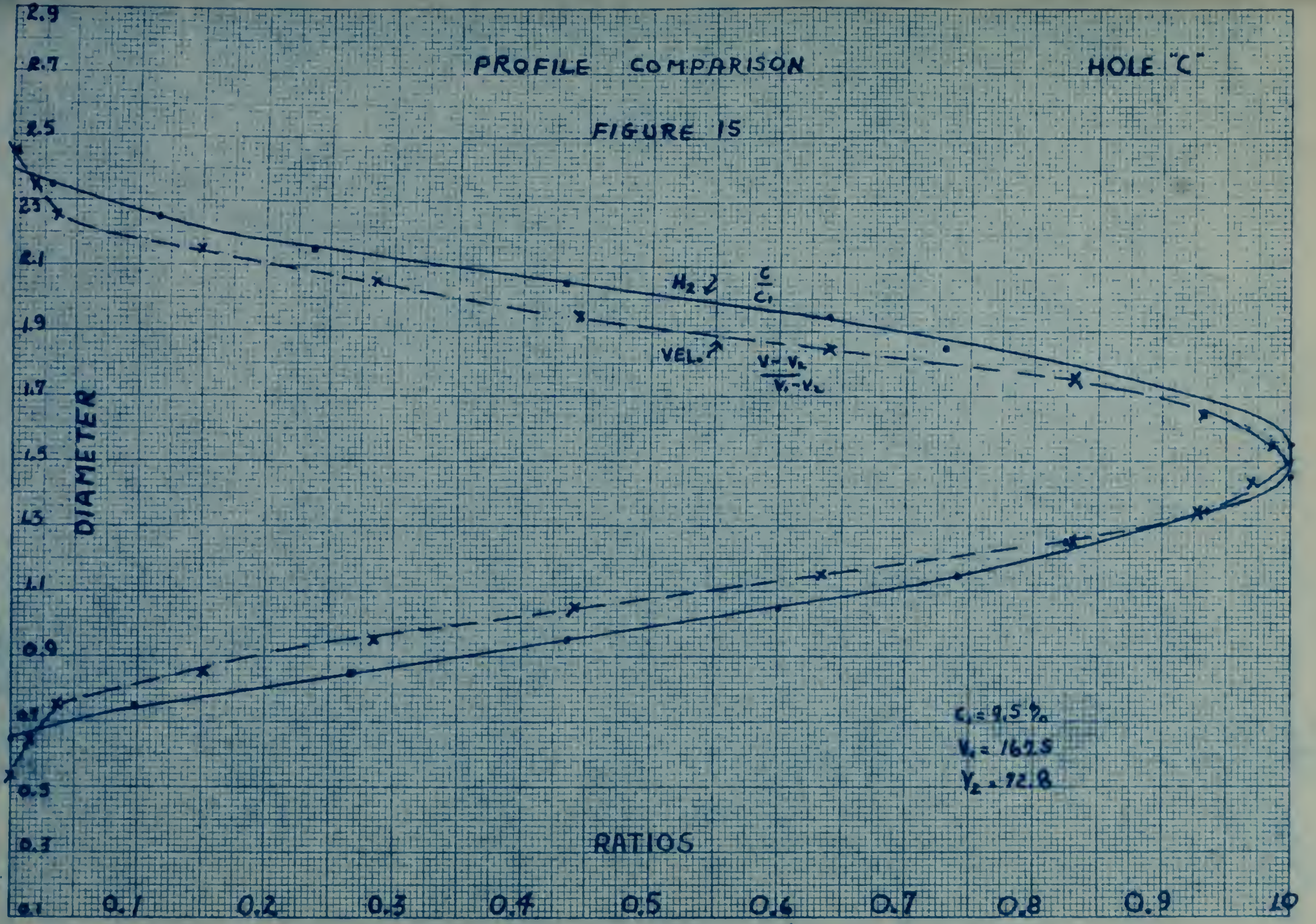
PROFILE COMPARISON
HOLE "C"
FIGURE 15
DIAMETER
RATIOS
VEL.
$\frac{V-V_2}{V_1-V_2}$
$\frac{C}{C_1}$
$C_1 = 9.5\ ?_0$
$V_1 = 162.5$
$V_2 = 72.8$
2.9
2.7
2.5
2.3
2.1
1.9
1.7
1.5
1.3
1.1
0.9
0.7
0.5
0.3
0.1
0.1
0.2
0.3
0.4
0.5
0.6
0.7
0.8
0.9
1.0

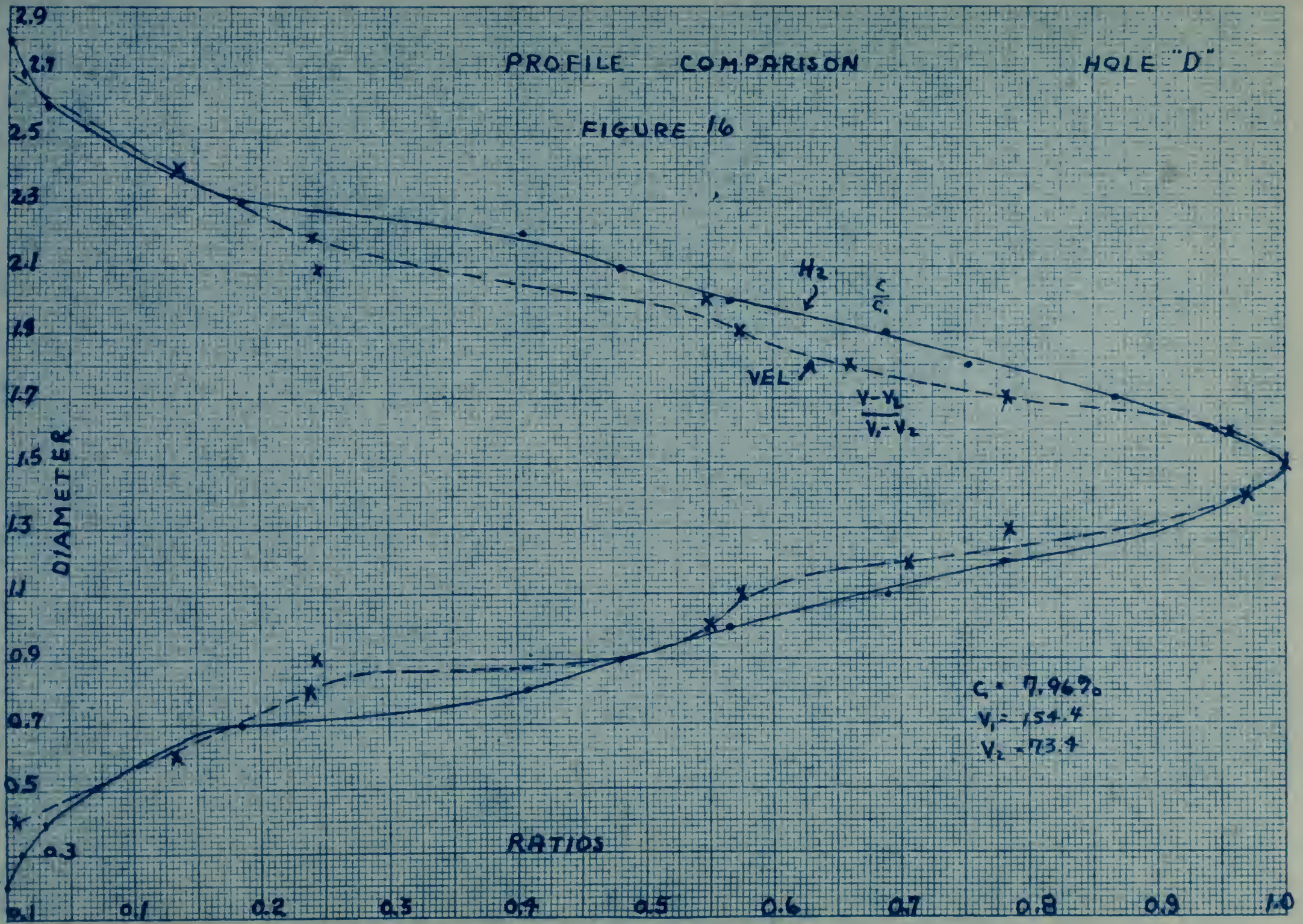
PROFILE COMPARISON HOLE "D"
FIGURE 16
DIAMETER
RATIOS
H_2
$\frac{c}{c_1}$
VEL
$\frac{V-V_2}{V_1-V_2}$
$C_1 = 7.962_0$
$V_1 = 154.4$
$V_2 = 73.4$
2.9
2.7
2.5
2.3
2.1
1.9
1.7
1.5
1.3
1.1
0.9
0.7
0.5
0.3
0.1
0.2
0.3
0.4
0.5
0.6
0.7
0.8
0.9
1.0

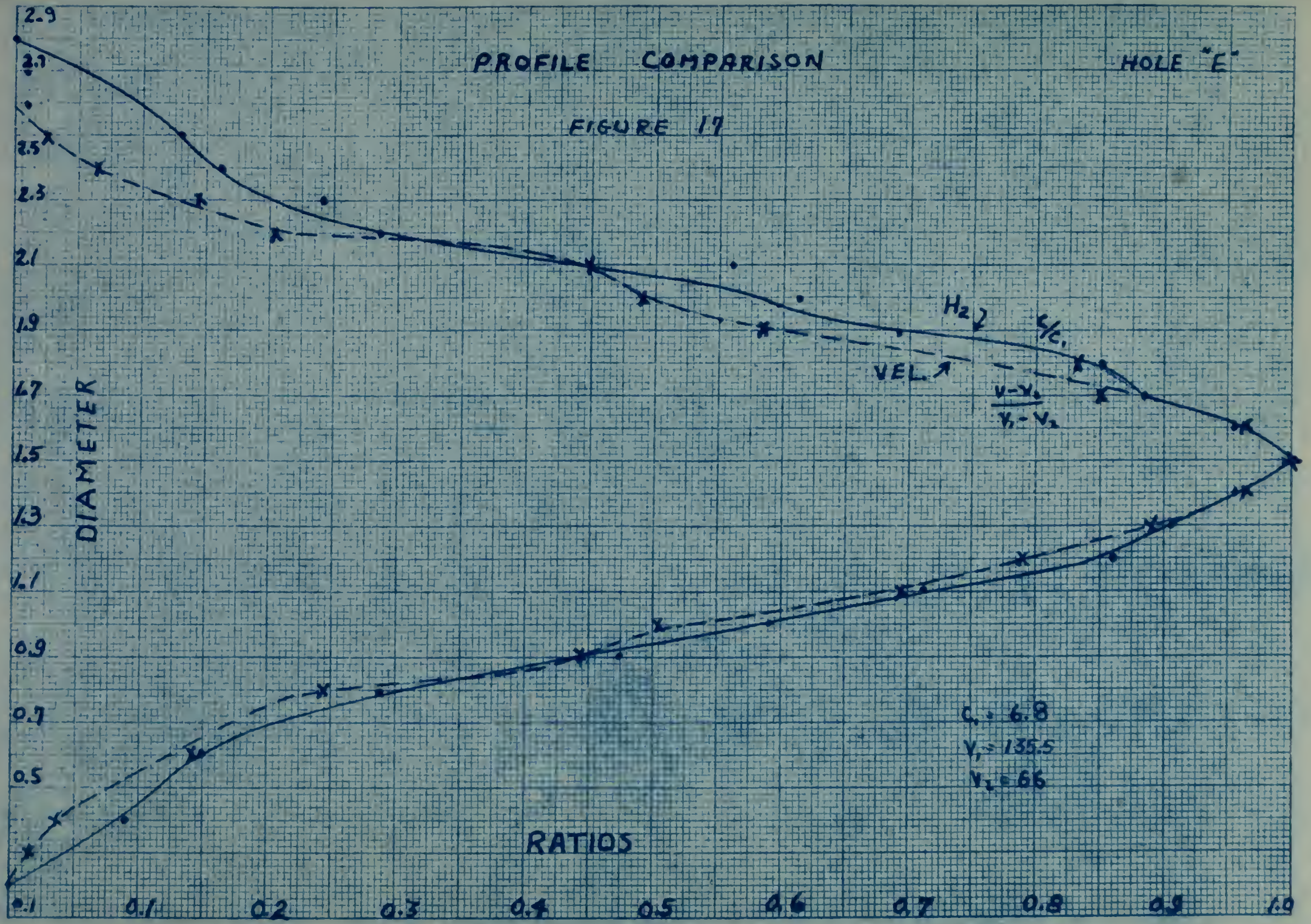
PROFILE COMPARISON
HOLE "E"
FIGURE 17
DIAMETER
RATIOS
H_2
ℓ/ℓ_1
VEL.
$\frac{v-v_2}{v_1-v_2}$
$C_1 = 6.8$
$V_1 = 135.5$
$V_2 = 66$
2.9
2.7
2.5
2.3
2.1
1.9
1.7
1.5
1.3
1.1
0.9
0.7
0.5
.1
0.1
0.2
0.3
0.4
0.5
0.6
0.7
0.8
0.9
1.0

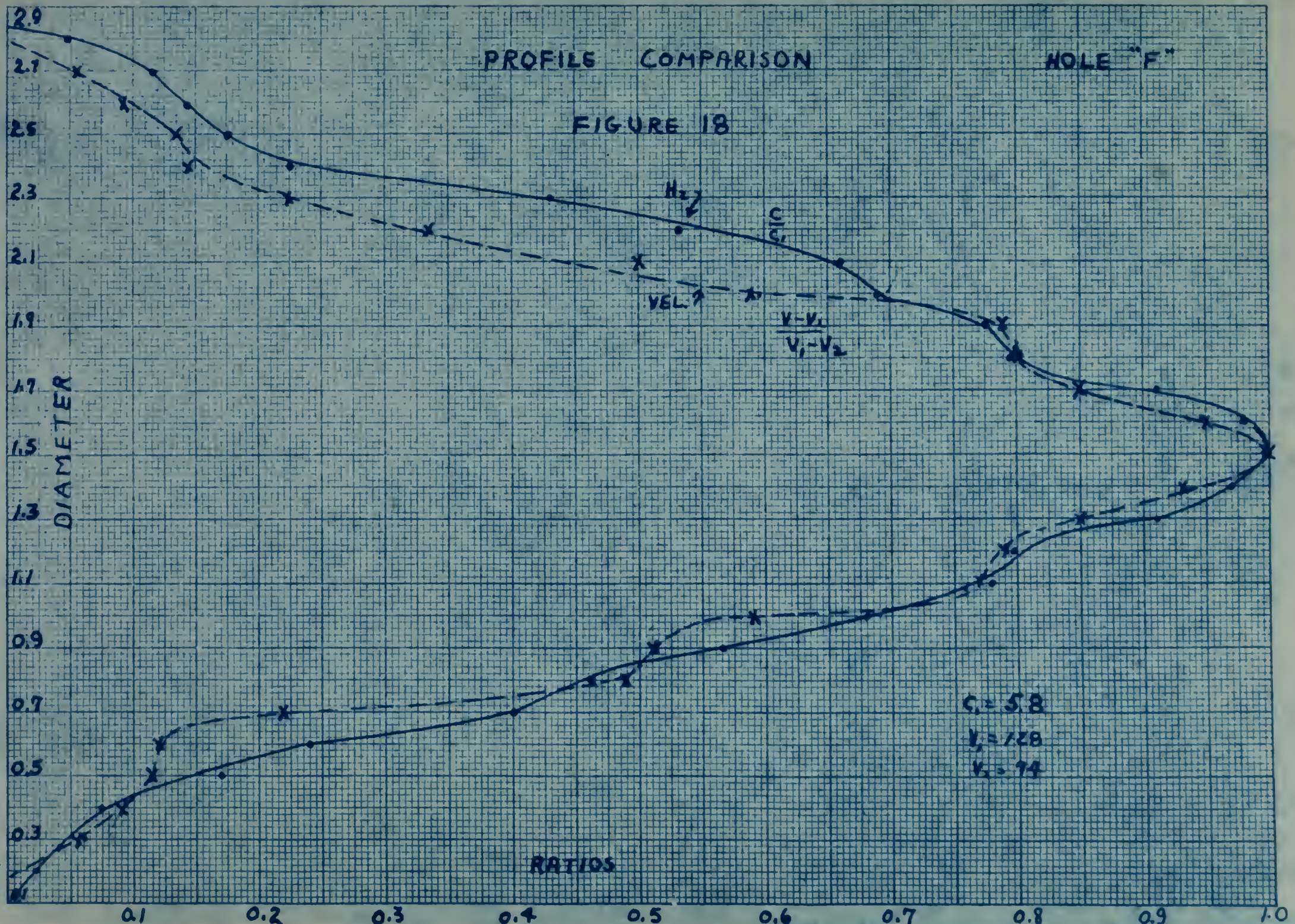
PROFILE COMPARISON
HOLE "F"
FIGURE 18
DIAMETER
RATIOS
VEL
$\frac{C}{C_1}$
$\frac{V-V_2}{V_1-V_2}$
$C_1 = 5.8$
$V_1 = 128$
$V_2 = 74$
2.9
2.7
2.5
2.3
2.1
1.9
1.7
1.5
1.3
1.1
0.9
0.7
0.5
0.3
0.1
0.2
0.3
0.4
0.5
0.6
0.7
0.8
0.9
1.0

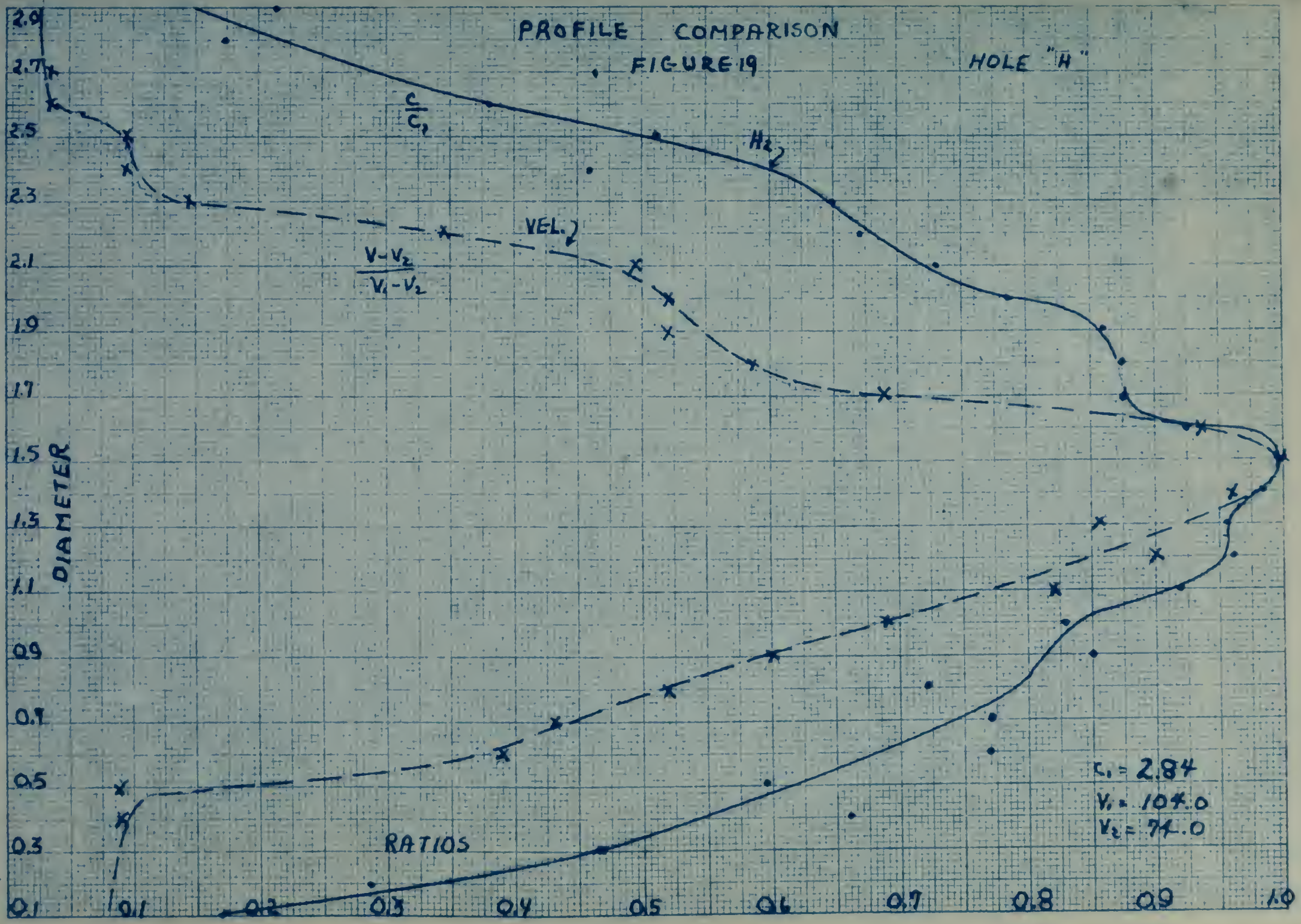
PROFILE COMPARISON
FIGURE 19
HOLE "H"
$\frac{C}{C_1}$
H_2
VEL.
$\frac{V-V_2}{V_1-V_2}$
DIAMETER
RATIOS
2.9
2.7
2.5
2.3
2.1
1.9
1.7
1.5
1.3
1.1
0.9
0.7
0.5
0.3
0.1
0.1
0.2
0.3
0.4
0.5
0.6
0.7
0.8
0.9
1.0
C_1 = 2.84
V_1 = 104.0
V_2 = 74.0

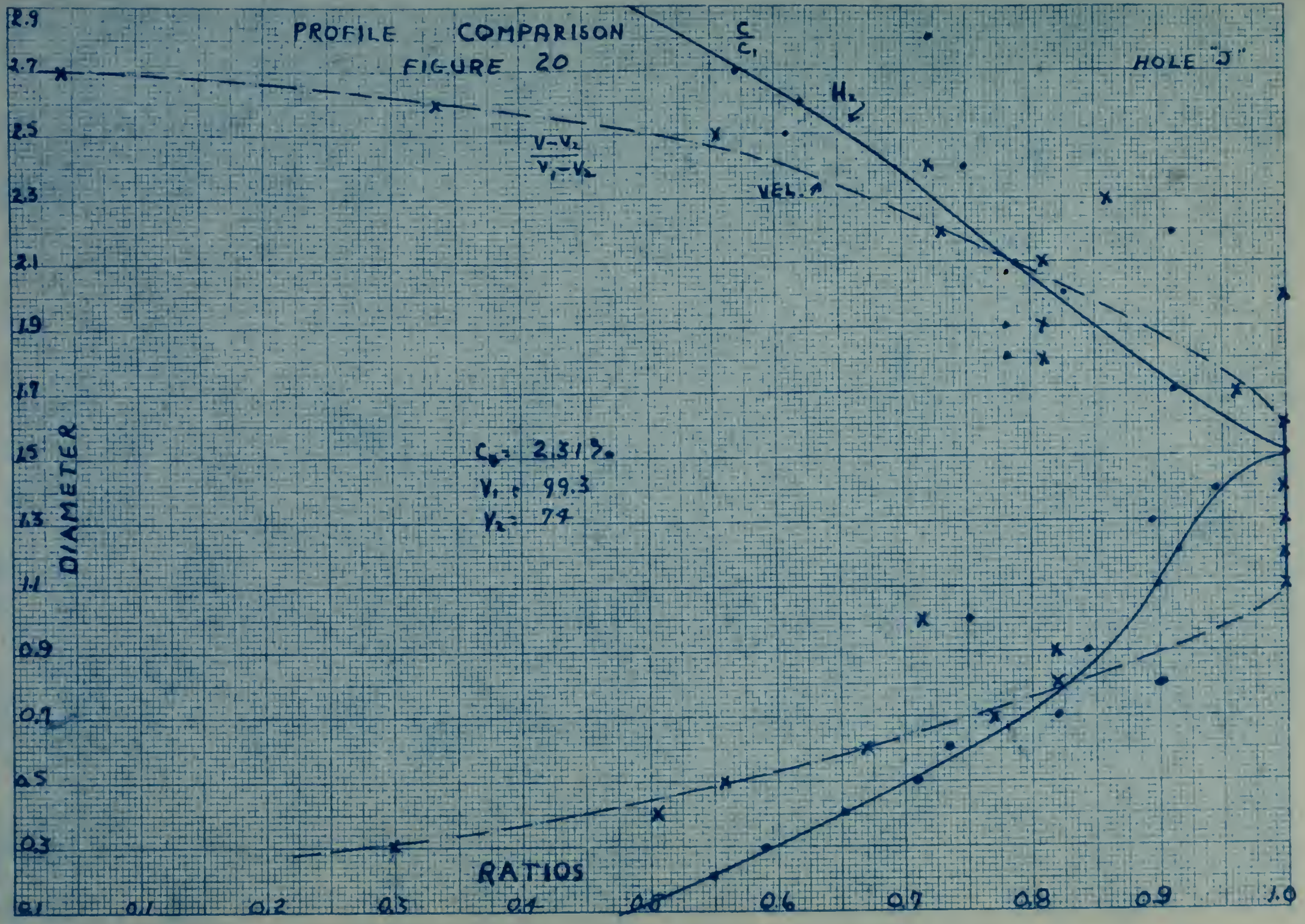
PROFILE COMPARISON
FIGURE 20
HOLE "J"
C/C1
H2
V-V2 / V1-V2
VEL.
C2 = 2.312
V1 = 99.3
V2 = 74
DIAMETER
RATIOS
2.9
2.7
2.5
2.3
2.1
1.9
1.7
1.5
1.3
1.1
0.9
0.7
0.5
0.3
0.1
0.2
0.3
0.4
0.6
0.7
0.8
0.9
1.0

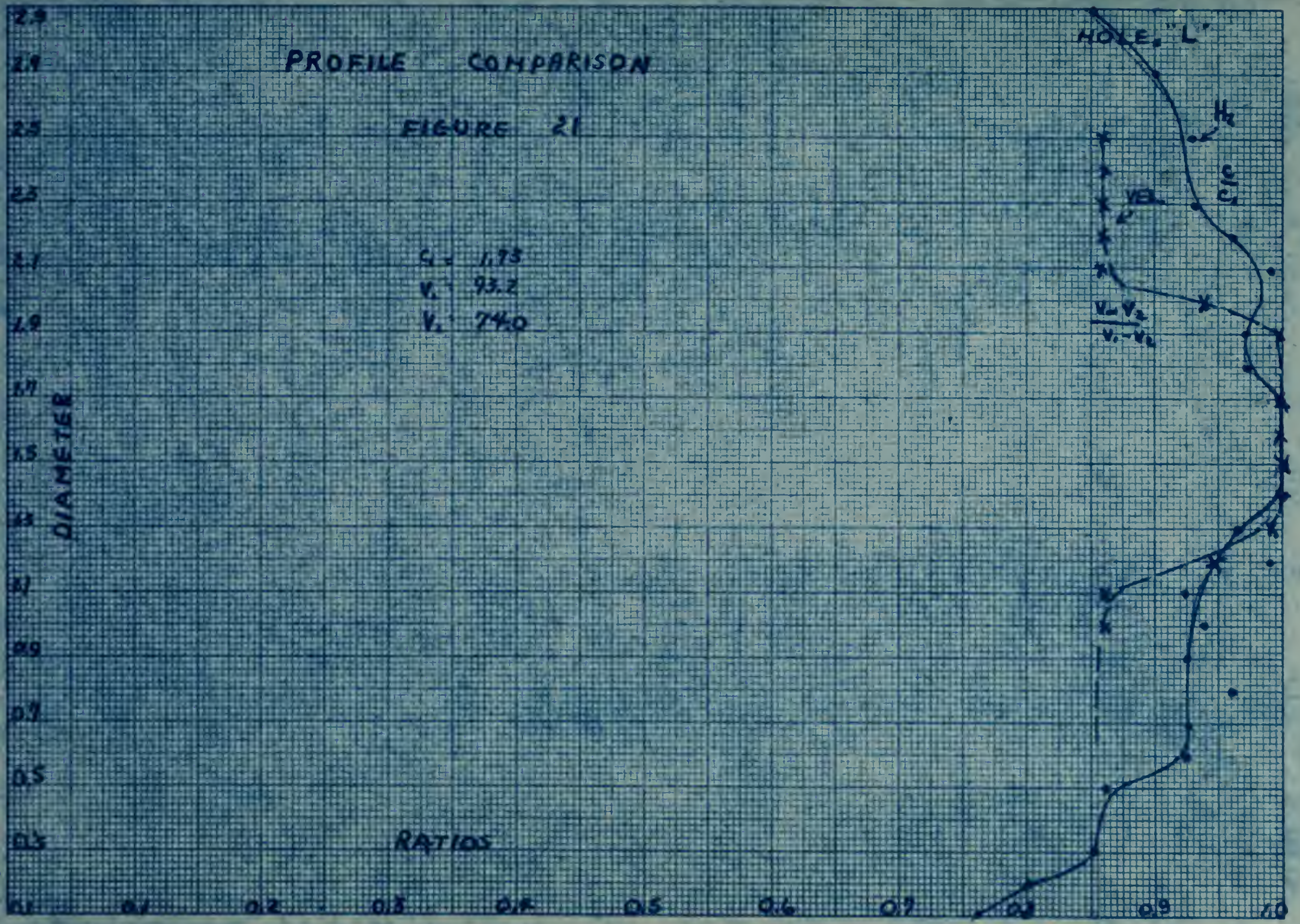
PROFILE COMPARISON
FIGURE 21
HOKE "L"
$C_L = 1.73$
$V_L = 93.2$
$V_t = 74.0$
DIAMETER
RATIOS
2.9
2.1
2.5
2.3
2.1
1.9
1.7
1.5
1.3
1.1
0.9
0.7
0.5
0.3
0.1
0.2
0.3
0.4
0.5
0.6
0.7
0.8
0.9
1.0

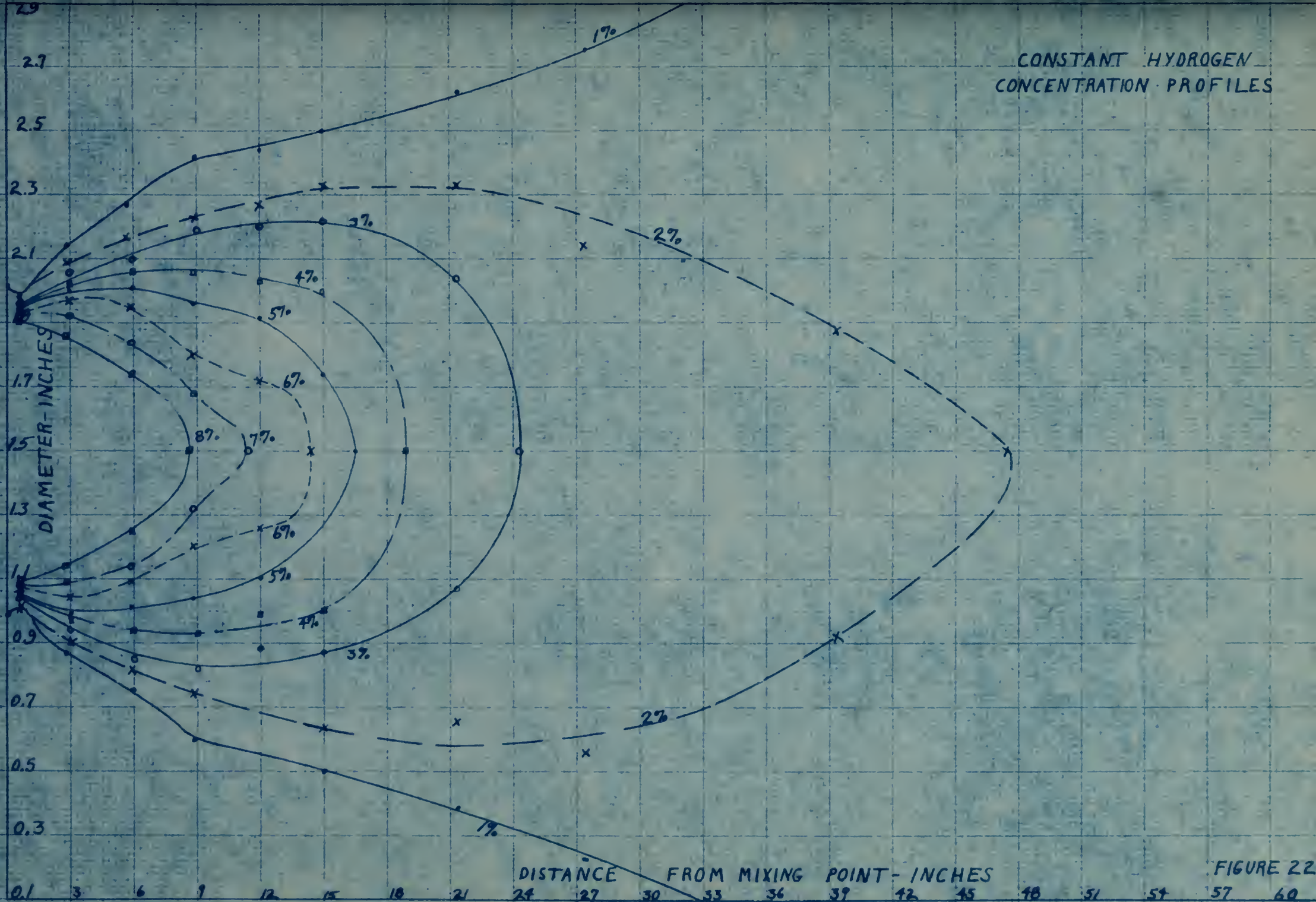
CONSTANT HYDROGEN CONCENTRATION PROFILES
DIAMETER-INCHES
DISTANCE FROM MIXING POINT - INCHES
1%
2%
2%
3%
4%
5%
6%
6%
7%
8%
0.1
0.3
0.5
0.7
0.9
1.1
1.3
1.5
1.7
2.1
2.3
2.5
2.7
2.9
3
6
9
12
15
18
21
24
27
30
33
36
39
42
45
48
51
54
57
60

FIGURE 22

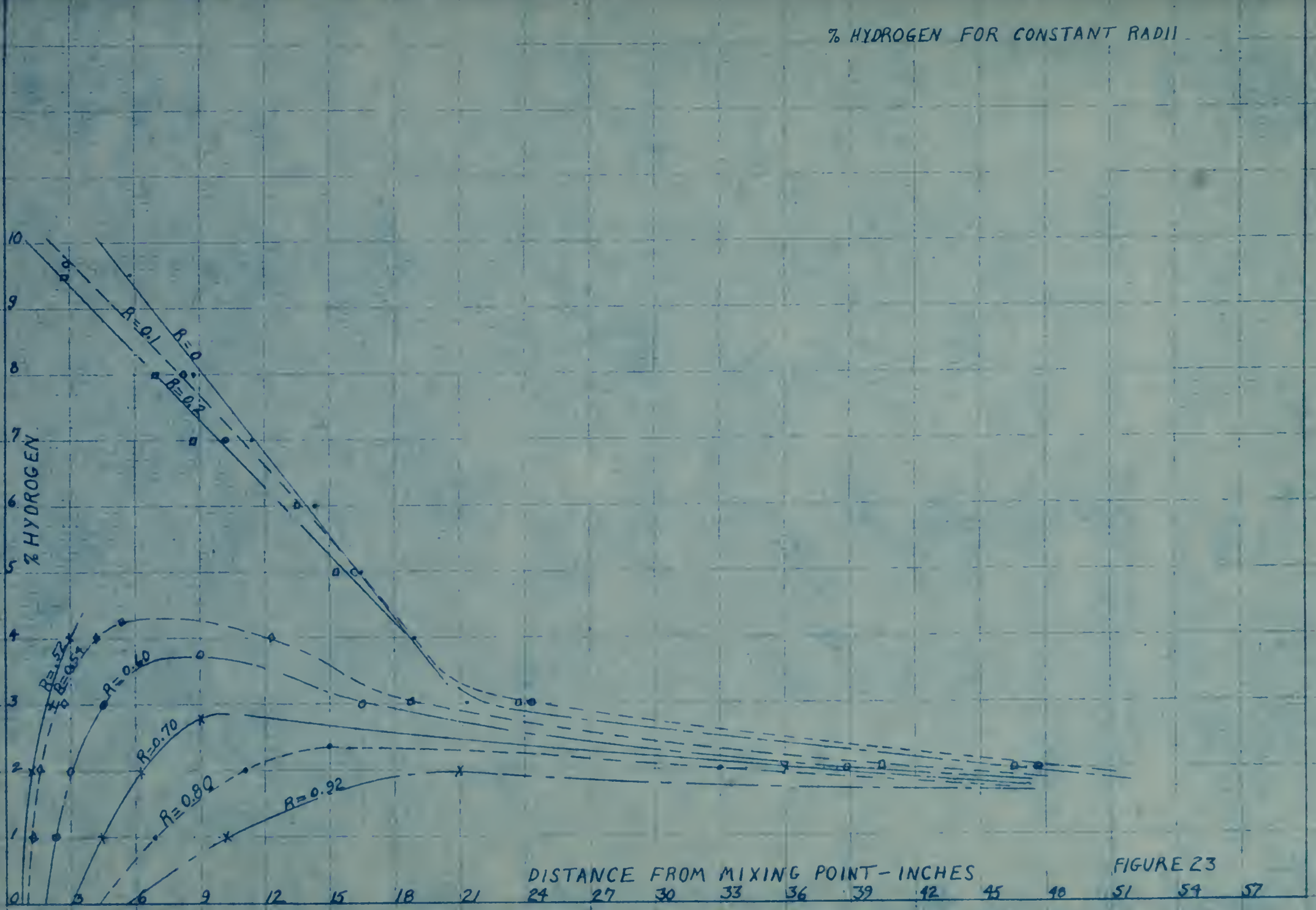
% HYDROGEN FOR CONSTANT RADII
% HYDROGEN
DISTANCE FROM MIXING POINT - INCHES
R=0
R=0.1
R=0.2
R=.52
R=0.53
R=0.60
R=0.70
R=0.80
R=0.92
0
3
6
9
12
15
18
21
24
27
30
33
36
39
42
45
48
51
54
57
1
2
4
5
7
8
10

FIGURE 23

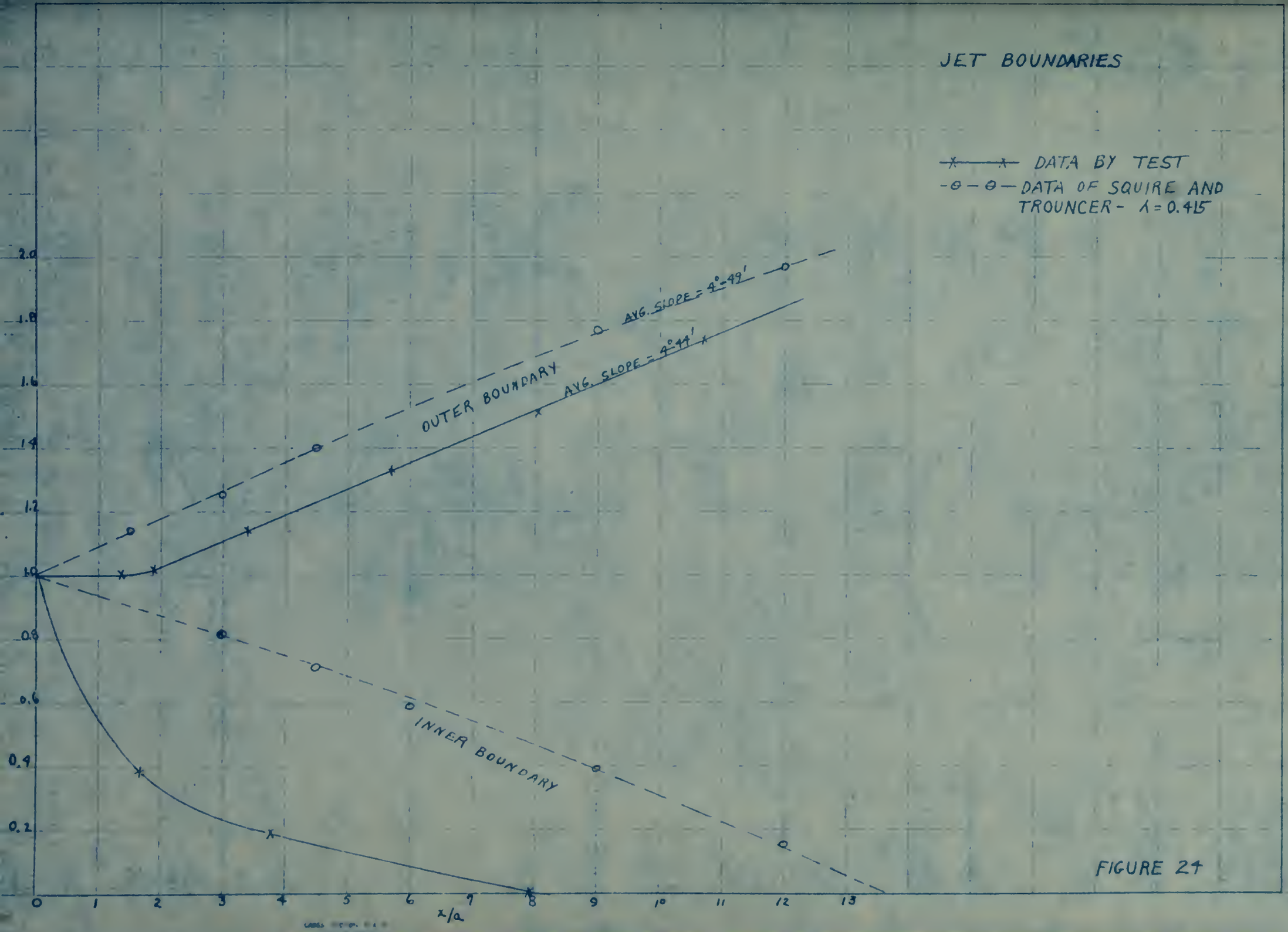
JET BOUNDARIES
DATA BY TEST
DATA OF SQUIRE AND TROUNCER - λ = 0.415
OUTER BOUNDARY
AVG. SLOPE = 4°-49'
AVG. SLOPE = 4°44'
INNER BOUNDARY
2.0
1.8
1.6
1.4
1.2
1.0
0.8
0.6
0.4
0.2
0
1
2
3
4
5
6
7
8
9
10
11
12
13
x/a

FIGURE 24

CHAPTER VIII

Discussion of Results

The hydrogen concentration profiles, Figures 8 and 9, indicate that under the conditions specified for these tests in Chapter VI:

1) A definite concentration peak exists for each traverse, rather than a flat profile across the center of the traverse.

2) For traverses near the mixing point, the sides of the profiles are almost perfectly straight lines.

3) At distances greater than ten diameters of the small jet from the mixing point, definite shoulders exist in the profiles in the outer mixing region. This may be explained by wall interference with the mixing process. There seems to be a definite qualitative correlation between these shoulders on the concentration profiles, and those on the velocity profiles.

4) At a distance of approximately 60 diameters of the initial jet, the mixing has reached a quasi-steedy state for which the concentration profiles at all sections are similar. That is, mixing is relatively complete.

5) At intermediate distances from the mixing point, i.e., holes H, J and K the concentration profile was so distorted by local turbulence that true symmetry about

the axis was lost.

The velocity profiles, Figures 10, 11, and 12, indicate that:

1) A definite base velocity exists in the annulus outside the core of mixture ejected from the small pipe. This velocity was assumed to be 74 ft/sec.

2) At distances up to 6 diameters from the mixing point, the velocity profiles, like the concentration profiles, have almost perfectly straight sides.

3) At points greater than 6 diameters, shoulders similar to those on the concentration profiles appear on the velocity profiles.

4) By the time hole J is reached, at 39 diameters, the variation of the maximum velocity to the mean velocity is roughly 7.5%.

When the hydrogen concentrations and velocities are plotted on a dimensionless basis as in Figures 13 to 21, indications are that:

1) The two profiles are qualitatively similar within the mixing region where wall effect is not evidenced. Quantitatively, the velocity profiles always lie somewhat inside the concentration profiles. This may be explained by the fact that when the mixture leaves the small pipe, there is already a well developed velocity profile present, whereas the concentration profile is perfectly flat That is, in the boundary regions very near the walls of the one

inch pipe the velocity is much less than the maximum velocity, but the hydrogen content is equal to the maximum due to the fact that there are two 90 degree bends and 20 feet of pipe between the entrance of the hydrogen and the exit of the mixture. It is believed that this definitely insured perfect mixing in the small pipe.

2) At distances greater than 21 diameters, there is little similarity between the dimensionless profiles. This is probably due to: (a) The interference of the walls, (b) The assumption of 74 ft/sec as a base velocity for comparison purposes when no definite velocity plateau existed which assumption may not be valid, (c) The fact that the velocity ratio is so sensitive to slight errors in experimental data since it is proportional to two values relatively near each other.

3) From the above plots, it is believed indicated that for traverses near the point of mixing, and if wall effect is not present, the velocity profiles and concentration profiles are similar.

A cross plot of hydrogen concentration curves, Figure 22, indicates that:

1) The surfaces of constant hydrogen concentration are fair.

2) The inner core boundary, if it were to follow the same contours as for points of lesser concentration, e.g., 8 percent, as it would logically be expected to do,

is a curved surface of small radius of curvature as shown in Figure 24, rather than one of large radius of curvature as deduced in the theoretical discussion of Squire and Trouncer (3).

3) Since I percent curves approach a straight line, it is reasonable to suppose that the outer boundary of the mixing region, that is, the 0 percent hydrogen curve, is a straight line, as shown by Figure 24. This agrees closely with the derived results of Squire and Trouncer.

4) At 16 diameters of the small pipe, the concentration has been reduced to one-half the original concentration along the axis.

5) At all points past 48 diameters, mixing is completed within 3 percent.

Figure 23, a plot of hydrogen concentrations versus mixing distance for constant radii, indicates that:

1) Within the primary core, the mixing rate is a constant up to 20 diameters, after which the rate decreases for a space of approximately 3 diameters, to a new, and almost constant rate over the remainder of the mixing range.

2) Mixing along both outer and inner boundaries is extremely rapid until approximately 22 diameters of the inner pipe, from which point it becomes comparatively slow, and almost constant for all radii. This is born out in Figure 22 by the close spacing of the contour lines until

24 diameters, after which they are widely spaced.

Figure 24, a dimensionless plot of the jet boundaries, was obtained by extrapolating the curves of Figure 23 to zero and ten percent hydrogen. The theoretical results of Squire and Trouncer (3) were obtained by a graphical interpolation of Figure 3, reference 3, for λ equals 0.415, and plotted on the same coordinates, thus obtaining the only check possible for the experimental results of this thesis. These curves show that:

1) The theoretical and experimental slopes of the outer boundary check within less than 2 percent. The experimental value of the average slope of the outer boundary of the cone of spread is 4° 44'. The theoretical value of Squire and Trouncer is 4° 49'.

2) The outer boundary as determined experimentally is displaced from the theoretical one in an axial direction. This is undoubtedly due to the effect of the finite thickness of the walls of the small pipe at the point of mixing. These walls are tapered inward on the outer surface of the pipe, thus giving an inward radial momentum to the outer stream just before the point of mixing is reached. This momentum must be overcome before the inner jet can actually begin to expand radially in the manner expected. The axial displacement may also be partially explained by the velocity profiles developed in both the inner and outer streams just before they reach the mixing point, whereas in

the theoretical analysis, a straight velocity profile is assumed.

3) As mentioned above, the inner boundary of the jet deduced by Squire and Trouncer does not agree with experimental results. This may be due to the fact that the experimental boundary was obtained by extrapolation, and only a few points could be obtained. However, since other results plotted in Figure 22 and mentioned above would also indicate a boundary similar to that shown as experimental results in Figure 24, it is considered likely that these results are correct for the conditions of this experiment.

CHAPTER IX

Conclusions

The principal conclusions of this thesis are that:

1) Mixing has reached a quasi-steady state by the time the stream has traveled 61 diameters of the small pipe from the point of mixing.

2) For sections near the point of mixing, and if wall effect is not present, velocity profiles and concentration profiles are similar if plotted on a dimensionless basis.

3) The outer boundary of the mixing region is a straight line of slope 40-44' for the velocity ratio $\lambda = 0.415$.

4) The inner boundary is the surface of revolution of a curve of comparatively small radius of curvature.

5) Mixing along both outer and inner boundaries is extremely rapid until about 22 diameters from the mixing point, where it becomes comparatively slow, and almost constant for all radii.

6) The thermo-conductivity cell is an extremely accurate and sensitive instrument for investigations of this kind.

CHAPTER X

Recommendations

It is recommended that:

1) This experiment be repeated for various velocity ratios.

2) A comparison between experimental and theoretical work be made with these various ratios.

3) The effect of turbulence promoters placed in the annulus of the outer pipe be investigated.

APPENDIX A

FLOW ACCOUNTABILITY

Total flow of the mixture past each traverse was checked by a comparison of the flow in an orifice in the 3 inch pipe (see Figure 7) with a point by point mass flow integration at the traverse in question.

The flow integration for three representative traverses, holes "A", "C", and "F" are shown in Figure "a", and a sample calculation for flow through the orifice is shown in the Sample Calculation Sheet which follows.

The flow as calculated by the flow integration across the traverses, equation (4), is:

Hole "A" 0.295 lbs./ sec.

Hole "B" 0.298 lbs./ sec.

Hole "C" 0.299 lbs./ sec.

The flow as calculated by orifice meter, equation (1), is:

$W_3 = 0.302$ lbs./ sec.

The maximum variation between orifice and integration is less than 2.5%, and the maximum variation between mass flow integration across comparable traverses is 1.5%.

The hydrogen mass flow past each traverse was checked by a comparison of the point hydrogen mass flow integration, equation (5), with the hydrogen flow issuing from the 1" pipe as measured by the mass ratio of hydrogen to air in

the 1' pipe and the mass flow of air through the orifice in the 1" pipe (equations 2 and 3).

The flow as calculated by the integration across the traverses, equation (5), is:

Hole A .328 x 10^{-3} lbs./ sec.

Hole B .337 x 10^{-3} lbs./ sec.

Hole C .360 x 10^{-3} lbs./ sec.

As calculated by equations 2 and 3 the flow is:

~~.410~~ .408 x 10^{-3} lbs./ sec.

The maximum variation between orifice measurements and integrations is 24%, and the maximum variation between hydrogen flow integrations across comparable traverses is 9.5%.

This large variation in flow rates could be due to the following causes:

a.) When the orifice was broken down it was found that large amounts of sediment had collected in the throat thereby effectively reducing the area.

b.) The assumption that the hydrogen density across the one inch pipe at the exit was uniform may not be valid.

The fact that the hydrogen flow across traverses at holes "A" and "B" checked closely with each other as it did for other holes on which data was checked, indicates that the hydrogen measuring device used was consistent and probably correct within the limits expected.

SAMPLE CALCULATION

A_1 area of orifice in 1" pipe (in.^{2})

A_3 area of orifice in 3" pipe (in.^{2})

K constant (Reference 4)

P_1 pressure before orifice in 1" pipe (lbs./ in.^{2})

ΔP pressure differential across orifice in 3" pipe (lbs./ in.^{2})

ρ density of fluid mixture at orifice in 3" pipe (lbs./ft^3)

ρ_M density of fluid mixture at any point in traverse (lbs./ ft.^{3})

R radius to any point in 3" pipe (inches)

T absolute temperature of air at orifice in 1" pipe (^oF abs)

V_M velocity of fluid mixture at any point in traverse (ft./sec.)

W_1 total air flow through orifice in 1" pipe (lbs./ sec.)

W_3 total mass flow at orifice in 3" pipe (lbs./ sec.)

W_M total hydrogen flow at a traverse (lbs./ sec.)

W_o total hydrogen flow at outlet of 1" pipe (lbs./ sec.)

W_T total mass flow at traverse (lbs./ sec.)

X mass ratio of hydrogen to air at any point in traverse

X_o mass ratio of hydrogen to air at outlet of 1" pipe

Y constant (reference 4)

$$W_3 = 0.668\ A_3\ KY\sqrt{\Delta P \rho} \qquad \text{(Reference 4)} \qquad (1)$$

$$W_1 = 0.53\ \frac{A_1\ P_1}{\sqrt{T}} \qquad \text{(Fleigner's Equation)} \qquad (2)$$

$$W_o = X_o\ W_1 \qquad (3)$$

$$W_T = \frac{\pi}{144} \int_0^R \rho_M V_M \, d(R^2) \qquad (4)$$

$$W_H = \frac{\pi}{144} \int_0^R \rho_M V_M X \, d(R^2) \qquad (5)$$

EXAMPLE:

Hole "A" Total Flow

$W_3 = .668 \times 3.57 \times .7 \times .99 \sqrt{.48 \times .0706} = 0.302$ lbs/sec.

$W_T = \frac{\pi}{144} \int_0^R \rho_M V_M \, d(R^2) = 0.295$ lb./sec. (Figure "a")

$\frac{W_3}{W_T} = 1.023$ (2.3 % discrepancy)

Hole "A" Hydrogen Flow

$W_1 = 0.53 \times \frac{.0285 \times 90.2}{\sqrt{580}} = .0566$ lbs./ sec.

$W_o = .00723 \times .0566 = .000408$ lbs./ sec.

$W_H = .000328$ lbs./ sec. (Figure "b")

$\frac{W_o}{W_H} = 1.24$

TOTAL FLOW ACCOUNTABILITY

$$W_T = \frac{\pi}{144} \int_0^R \rho_m V_m \, d(R^2)$$

$W_A = .295$ #/s
$W_C = .298$ #/s
$W_F = .299$ #/s

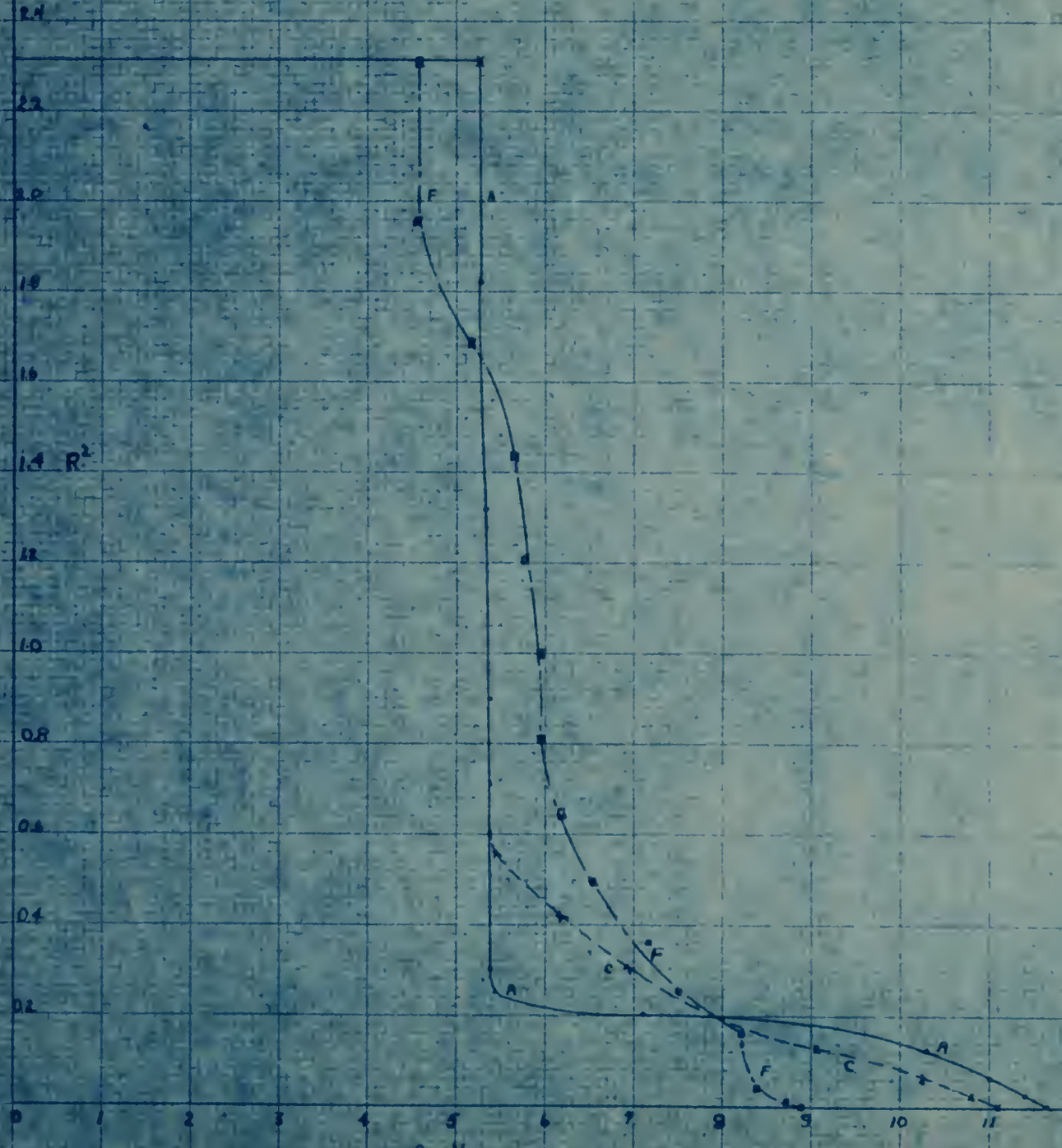

FIGURE "a"

HYDROGEN ACCOUNTABILITY

$$\omega_H = \frac{\pi}{144} \int_0^R \rho_m V_m X \, d(R^2)$$

HOLE A: $\omega_H = .328 \times 10^{-3}$ #/s

HOLE C: $\omega_H = .337 \times 10^{-3}$ #/s

HOLE F: $\omega_H = .360 \times 10^{-3}$ #/s

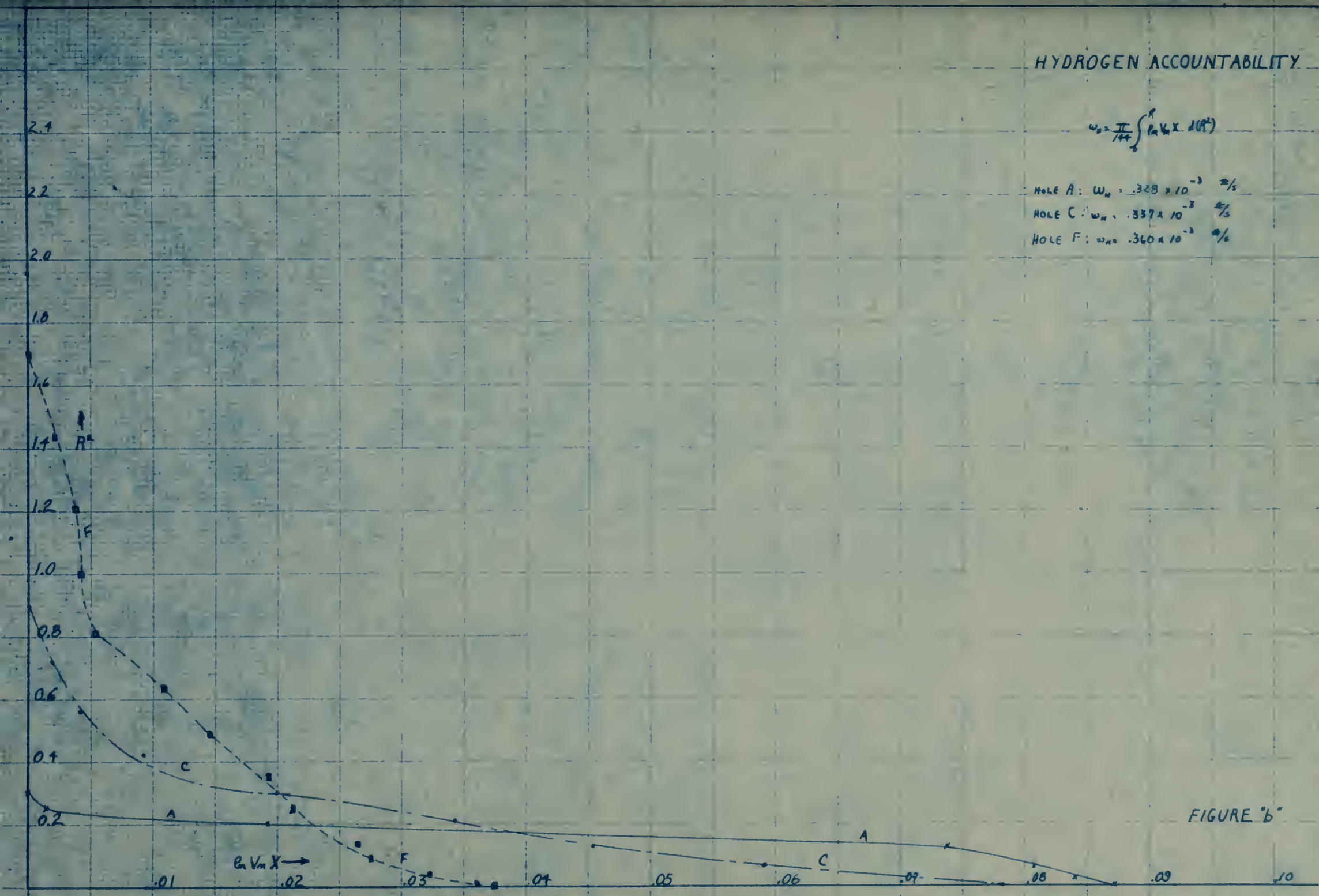

FIGURE "b"

APPENDIX B

Data Sheets and Sample Calculations

DATA SHEET I

CALIBRATION RUNS

Zero	% H_2	Run 1 R	Run 1 ΔR	Run 2 R	Run 2 ΔR
1016.85	50	1229.0	212.15	1229.	212.15
1016.44	25	1150.3	133.86	1150.3	133.21
1016.03	12.5	1092.25	76.22	1092.65	76.62
1015.62	6.25	1057.0	41.38	1056.65	41.03
1015.2	3.125	1037.25	22.05	1037.05	21.85
1016.4	1.567	1027.85	11.45	1027.25	10.85
1016.34	.781	1022.25	5.91	1021.85	5.51
1016.28	.3905	1019.2	2.92	1019.1	2.82
1016.22	.1952	1017.6	1.38	1016.9	1
1016.17	.0976	1016.85	.68	1016.45	
1016.11	.0488	1016.55	.44	1016.40	
1016.05	.0244	1016.55			

Zero	% H_2	Run 3 R	Run 3 ΔR	Run 4 R	Run 4 ΔR
1016.6	33.33	1182.6	166.	1182.35	165.75
1016.36	16.67	1114.05	97.7	1114.2	97.85
1016.12	8.33	1070.55	54.43	1069.9	53.78
1015.88	4.17	1044.4	28.52	1044.25	28.37
1015.65	2.083	1030.5	14.85	1030.5	14.85
1015.73	1.042	1023.45	7.72	1023.25	7.52
1015.81	.521	1019.85	4.04	1019.85	4.04
1015.90	.260	1017.85	1.95	1017.75	1.85
1015.98	.13	1016.8	.82	1016.8	.82
1016.07	.065	1016.45	.38	1016.5	.44

DATA SHEET II

Distance of Needle Tip of each hole from junction of two streams.

Hole	Distance (inches)	Hole	Distance
A	0.55	G	21.42
B	2.86	H	27.42
C	5.86	J	39.42
D	8.86	K	51.42
E	12.05	L	61.42
F	15.05		

SAMPLE CALCULATION

Hole C, Traverse Reading 1.5 inches.

To find velocity V:

$$M.W. = (2)x(\%\ H_2) + (29)x(\%\ air)$$
$$= (2)x(9.33\%) + (29)x(90.67\%)$$
$$= 26.45$$

$$\rho_{mix} = \frac{(p)x(144)}{(R)x(T)} \times (M.W.)$$
$$= \frac{(14.6)x(144)x(26.45)}{(1545)x(543)}$$
$$= 0.0661\ lb/ft^3$$

$$V = \sqrt{\frac{(2g)x(62.4)}{(12)}} \cdot \sqrt{\frac{Pitot\ Reading}{mix}}$$
$$= 18.25\sqrt{\frac{Pitot}{\rho mix}} = 18.25\sqrt{\frac{5.55}{0.0661}}$$
$$= 167\ ft/sec.$$

DATA SHEET III

HOLE A

Zero = 1016.2; Bar.= 30.07; T = 91; Δp in 3" = 1.11ft.
p (static) in 3" = .21'.

Traverse	R	% H_2	Pitot	V	c/c_1	$\frac{V - V_2}{V_1 - V_2}$
2.8	1016.2	0	1.15	73.0	0	0
2.6	1016.2	0	1.18	74.1	0	0
2.4	1016.2	0	1.2	74.6	0	0
2.2	1016.2	0	1.2	74.6	0	0
2.1	1016.35	0	1.2	74.6	0	0
2.0	1016.25	0	1.22	74.6	0	0
1.95	1018.55	.3		75.4	.0303	.0078
1.9	1042.5	3.8	2.15	102.0	.384	.267
1.8	1076.8	9.44	4.8	156.5	.955	.80
1.7	1078.8	9.7	5.5	167.5	.980	.906
1.6	1078.8	9.7	5.9	173.5	.980	.965
1.5	1079.1	9.86	6.15	177.0	.998	1.0
1.4	1078.8	9.7	6.15	177.0	.998	1.0
1.3	1078.5	9.65	6.0	174.5	.975	.974
1.2	1077.1	9.5	5.65	169.5	.961	.925

DATA SHEET IV

HOLE B

Zero: 1016.9; Bar. = 29.86; T = 91; p in 3" = 1.11';
p (static) in 3" = .21'.

Traverse	R	% H_2	Pitot	V	c/c_1	$\frac{V - V_2}{V_1 - V_2}$
2.9	1016.95	0	1.05	70.2	0	0
2.8	1017.2	.04	1.15	73.5	.004	0
2.7	1017.0	.015	1.15	73.5	0	0
2.6	1016.8	0	1.15	73.5	0	0
2.5	1016.9	0	1.15	73.5	0	0
2.4	1016.8	0	1.15	73.5	0	0
2.3	1017.0	.015	1.15	73.5	0	0
2.2	1021.0	.53	1.15	73.5	.053	0
2.1	1029.7	1.8	1.15	74.0	.179	.0049
2.0	1051.75	5.23	1.35	81.4	.523	.0776
1.9	1066.25	7.56	2.35	108.5	.755	.344
1.8	1076.65	9.3	3.90	141.5	.929	.662
1.7	1079.1	9.75	5.25	164.0	.974	.884
1.6	1080.45	10.00	5.95	175.0	.996	.983
1.5	1080.65	10.03	6.1	176.0	1.	1.
1.45	1080.4	10.02			.999	
1.4	1079.6	9.88	6.1	176.0	.986	1.
1.3	1079.5	9.85	6.0	175.5	.985	.995
1.2	1076.25	9.26	5.7	171.0	.925	.95
1.1	1065.5	7.48	4.5	150.0	.746	.745
1.0	1051.7	5.25	3.0	121.0	.524	.46
.9	1029.0	1.74	1.75	91.2	.174	.173

DATA SHEET V

HOLE C

Zero = 1017.35; Bar. = 29.86; T = 83; Δp in 3" = 1.11;
p (static) in 3" = .21.

Traverse	h	% Ho	Pitot	V	c/c1	$\frac{V - V_2}{V_1 - V_2}$
2.9	1018.15	.115	1.15	72.8	0	0
2.8	1017.35	0	1.15	72.8	0	0
2.7	1017.35	0	1.15	72.8	0	0
2.6	1017.35	0	1.15	72.8	0	0
2.5	1017.35	0	1.15	72.8	0	0
2.4	1017.35	0	1.15	72.8	0	0
2.3	1021.4	.52	1.2	74.4	.0558	.0167
2.2	1025.2	1.075	1.25	76.0	.1155	.0334
2.1	1033.2	2.225	1.6	87.0	.238	.148
2.0	1045.0	4.025	2.1	100.	.431	.264
1.9	1056.05	5.95	2.7	115.	.637	.441
1.8	1061.85	6.8	3.65	134.	.728	.639
1.7	1067.7	7.73	4.7	152.5	.829	.831
1.6	1074.85	8.78	5.25	162.	.942	.931
1.5	1077.15	9.33	5.55	167.	1.	.984
1.45	1077.3	9.35	5.6	167.5	1.	1.
1.4	1077.2	9.34	5.47	165.8	1.	.97
1.3	1076.6	8.7	5.2	161.5	.936	.926
1.2	1067.5	7.7	4.7	152.5	.825	.832
1.1	1062.9	6.9	3.6	133.5	.739	.633
1.0	1054.0	5.5	2.7	115.	.59	.441
.9	1045.15	4.05	2.1	100.	.434	.284
.8	1035.3	2.52	1.6	87.	.269	.148
.7	1024.2	.92	1.25	76.	.0985	.033
.6	1017.6	.025	1.2	74.4	0	.016
.5	1017.4	0	1.15	72.8	0	.016
.4	1017.4	0	1.15	72.8	0	.016
.3	1017.4	0	1.15	72.8	0	.016
.2	1017.4	0	1.15	72.8	0	.016
.1	1017.4	0	1.15	72.8	0	.016
0	1017.4	0	1.15	72.8	0	.016

DATA SHEET VI

HOLE D

Baro = 1016.6; Bal. = 29.86; T = 8[illegible] Δp in 3" = 1.11";
p (static) in 3" = .22!

Traverse	R	% H_2	Pitot	V	c/c_1	$\frac{V - V_2}{V_1 - V_2}$
2.9	1017.25	.08	1.05	70.1	0	0
2.8	1016.9	.035	1.15	73.4	.0044	0
2.7	1017.3	.09	1.15	73.4	.0112	0
2.6	1018.35	.23	1.17	73.9	.0283	.0061
2.5			1.21			
2.4	1024.3	1.075	1.52	84.5	.133	.137
2.3	1027.4	1.48			.184	
2.2	1036.9	2.87	1.8	93.0	.336	.242
2.1	1043.4	3.88	1.8	93.1	.481	.243
2.0	1047.45	4.55	2.85	118.0	.566	.55
1.9	1053.55	5.54	2.95	120.0	.688	.574
1.8	1056.7	6.05	3.25	127.0	.752	.66
1.7	1062.3	6.95	3.75	136.5	.863	.778
1.6	1066.2	7.6	4.5[illegible]	151.0	.944	.936
1.5	1069.2	8.08	4.75	154.4	1.	1.
1.4	1066.2	7.6	4.6	152.0	.944	.97
1.2	1059.0	6.28	3.25	126.5	.780	.654

DATA SHEET VII

HOLE E

Zero = 1016.4; Bar. = 30.07; T = 83; Δp in 3" = 1.11;
p (static) in 3" = .22.

Traverse	R	% H_2	Pitot	V	c/c_1	$\frac{V - V_2}{V_1 - V_2}$
2.9	1016.4	0	.75	60.5	0	0
2.7	1016.6	.05	.95	65.5	.0073	0
2.6	1016.6	.05	.95	65.5	.0073	.0241
2.5	1022.7	.88	1.0	67.7	.123	.0577
2.4	1024.0	1.11	1.1	70.7	.162	.144
2.3	1028.0	1.65	1.25	76.0	.241	.204
2.2	1030.1	1.95	1.40	80.2	.297	.449
2.1	1042.5	3.83	2.05	97.1	.358	.49
2.0	1044.3	4.18	2.12	100.	.611	.584
1.9	1048.0	4.73	2.70	113.5	.692	.778
1.8	1054.8	5.83	3.0	120.0	.852	.85
1.7	1056.3	6.06	3.25	125.	.885	.965
1.6	1059.3	6.53	3.65	133.	.955	1.
1.5	1061.2	6.85	3.80	135.5	1.	.965
1.4	1059.75	6.55	3.65	133.	.956	.89
1.3	1056.9	6.18	3.35	127.8	.904	.79
1.2	1054.3	5.88	3.05	121.	.859	.695
1.1	1049.1	4.88	2.75	114.4	.710	.504
1.0	1044.0	4.05	2.15	101.0	.592	.445
.9	1039.	3.25	2.0	97.0	.473	.246
.8	1030.4	2.0	1.5	83.1	.289	.0935
.6	1023.6	1.02	1.15	72.5	.149	.036
.4	1020.5	.63	1.05	69.2	.0912	.0144
.2	1016.4	0	1.0	67.0	0	0
0	1016.4	0	1.0	0	0	

DATA SHEET VIII

HOLE F

Zero = 1016.7; Bar. = 30.12; T = 81; Δp in 3" = 1.11';
p (static) in 3" = .2'.

Traverse	R	% H_2	Pitot	V	c/c_1	$\frac{V - V_2}{V_1 - V_2}$
2.9	1016.9	.03	.85	62.	0	0
2.8	1018.7	.275	1.0	70.7	.0478	0
2.7	1021.8	.67	1.3	77.0	.117	.0555
2.6	1022.9	.83	1.35	79.0	.144	.0925
2.5	1024.15	1.02	1.45	81.5	.177	.138
2.4	1026.1	1.3	1.45	81.8	.225	.144
2.3	1034.8	2.47	1.6	86.0	.428	.222
2.2	1038.	3.08	1.8	92.1	.532	.334
2.1	1042.9	3.8	2.15	101.	.660	.50
2.0	1044.0	3.98	2.37	106.	.690	.59
1.9	1047.2	4.48	2.85	116.5	.775	.79
1.8	1047.9	4.6	2.87	117.5	.796	.80
1.7	1052.	5.26	3.0	120.	.910	.85
1.6	1054.3	5.65	3.25	125.5	.978	.95
1.5	1055.2	5.78	3.4	128.	1.	1.
1.4	1054.	5.6	3.25	124.5	.968	.93
1.3	1052.	5.26	3.0	120.	.910	.85
1.2	1047.7	4.6	2.88	117.	.795	.79
1.1	1047.2	4.5	2.80	115.8	.78	.77
1.0	1043.7	3.92	2.35	106.	.68	.59
.9	1039.8	3.28	2.15	101.5	.566	.51
.8	1035.9	2.68	1.8	100.5	.46	.49
.7	1033.5	2.34	1.6	86.0	.4	.22
.6	1025.9	1.38	1.4	80.5	.24	.15
.5	1024.2	.99	1.4	80.2	.172	.115
.4	1020.2	.43	1.35	78.9	.075	.09
.3	1019.5	.346	1.3	77.0	.06	.055
.2	1017.9	.13	.95	66.0	.022	0
.1	1016.9	0	.85	62.	0	0

DATA SHEET IX

HOLE G

Zero = 1017.35; Bar. = 29.92; T = 91; Δp in 3" = 1.11';
p (static) in 3" = .215'

Traverse	R	% H_2	Pitot	V	c/c_1	$\frac{V - V_2}{V_1 - V_2}$
2.9	1018.0	.085	.85	63.0	.0244	0
2.8	1019.2	.25	1.25	76.1	.069	.055
2.7	1029.7	1.72	1.50	83.8	.495	.254
2.6	1031.0	1.91	1.60	87.5	.55	.35
2.5	1028.4	1.53	1.80	91.8	.44	.46
2.4	1032.2	2.12	2.20	102.0	.61	.73
2.3	1034.5	2.42	2.25	103.	.7	.755
2.2	1034.4	2.42	2.25	103.	.7	.755
2.1	1039.4	3.13	2.25	103.	.93	.755
2.0	1034.6	2.42	2.30	104.2	.7	.79
1.9	1039.4	3.13	2.50	109.0	.93	.91
1.8	1041.4	3.45	2.60	111.5	.995	.975
1.7	1039.2	3.1	2.25	103.4	.89	.765
1.6	1039.5	3.15	2.75	115.0	.91	
1.5	1041.6	3.48	2.65	112.5	1.	1.
1.4	1039.8	3.2	2.65	112.5	.92	1.
1.3	1039.8	3.2	2.45	108.0	.92	.885
1.2	1038.6	3.18	2.45	108.0	.91	.885
1.1	1036.0	2.62	2.23	103.	.75	.755
1.0	1034.	2.35	2.13	101.2	.675	.72
.9	1035.7	2.58	2.15	101.2	.74	.72
.8	1034.2	2.38	2.0	97.2	.68	.6
.7	1032.4	2.10	1.75	90.6	.60	.43
.6	1030.4	1.82	1.6	87.5	.52	.35
.5	1024.4	.95	1.75	90.6	.27	.6
.4	1024.3	.94	1.4	81.0	.27	.18
.3	1024.6	.98	1.4	81.0	.28	.18
.2	1020.2	.37	1.2	74.5	.11	.013
.1	1019.5	.29	1.03	71.0	.09	.013

DATA SHEET X

HOLE H

Zero = 1018; Bar. = 30.08; T = 86; Δp in 3' = 1.11';
p (static) in 3" = .21'.

Traverse	R	% H_2	Pitot	V	c/c_1	$\frac{V - V_2}{V_1 - V_2}$
2.9	1022.8	.625	.75	58.8	.214	0
2.8	1021.9	.50	1.05	69.5	.173	0
2.7	1027.6	1.33	1.2	75.0	.465	.033
2.6	1026.	1.1	1.2	75.0	.38	.033
2.5	1028.4	1.45	1.26	76.8	.51	.093
2.4	1027.5	1.32	1.26	76.8	.46	.093
2.3	1031.3	1.86	1.3	78.4	.65	.147
2.2	1031.6	1.91	1.52	84.3	.67	.394
2.1	1033.	2.1	1.68	88.8	.73	.495
2.0	1034.	2.25	1.70	89.6	.785	.52
1.9	1035.5	2.46	1.7	89.6	.86	.52
1.8	1035.7	2.5	1.75	91.0	.874	.57
1.7	1035.7	2.5	1.90	94.6	.874	.69
1.6	1036.7	2.65	2.20	102.0	.925	.935
1.5	1038.2	2.86	2.3	104.0	1.	1.
1.4	1037.9	2.82	2.22	102.8	.985	.96
1.3	1037.2	2.73	2.10	99.6	.955	.854
1.2	1037.3	2.75	2.13	101.0	.960	.9
1.1	1036.6	2.63	2.05	98.5	.92	.82
1.0	1034.8	2.37	1.90	94.6	.83	.69
.9	1035.2	2.42	1.80	92.0	.85	.6
.8	1032.6	2.05	1.70	89.5	.72	.52
.7	1033.7	2.2	1.6	87.0	.77	.433
.6	1033.6	2.2	1.55	85.7	.77	.39
.5	1030.1	1.7	1.25	76.7	.595	.09
.4	1031.4	1.88	1.25	76.7	.66	.09
.3	1027.6	1.33	1.10	71.6	.465	0
.2	1024.1	.82	.90	64.5	.285	0
.1	1021.8	.5			.172	0

DATA SHEET XI

HOLE J

Zero = 1018; Bar. = 30.08; T = 86; Δp in 3' = 1.11';
p (static) in 3" = .21'.

Traverse	R	% H_2	Pitot	V	c/c_1	$\frac{V - V_2}{V_1 - V_2}$
2.9	1029.6	1.67	1.0	71.8	.72	.0396
2.8	1027.5	1.31	1.2	75.5	.57	.0396
2.7	1028.3	1.43	1.45	82.5	.62	.336
2.6	1028.2	1.40	2.0	96.8	.61	.506
2.5	1030.4	1.75	1.8	92.2	.75	.72
2.4	1031.8	1.93	1.95	95.8	.83	.86
2.3	1033.0	2.10	1.8	92.5	.91	.73
2.2	1031.0	1.83	1.9	94.5	.79	.81
2.1	1032.0	1.96	2.10	99.4	.85	1.0
2.0	1030.8	1.8	1.9	94.5	.78	.81
1.9	1030.9	1.81	1.9	94.5	.78	.81
1.8	1033.2	2.13	2.05	98.3	.92	.96
1.7	1031.8	1.94	2.10	99.3	.84	1.
1.6	1034.4	2.31	2.10	99.3	1.0	1.
1.5	1033.6	2.19	2.10	99.3	.945	1.
1.4	1032.9	2.07	2.10	99.3	.894	1.
1.3	1033.1	2.12	2.10	99.3	.915	1.
1.2	1033.5	2.17	2.10	99.3	.9	1.
1.1	1030.4	1.74	1.80	92.2	.75	.715
1.0	1032.0	1.96	1.9	94.6	.845	.8
.9	1033.0	2.10	1.9	94.6	.90	.82
.8	1031.6	1.91	1.85	93.5	.82	.77
.7	1030.2	1.71	1.75	91.0	.735	.67
.6	1029.9	1.66	1.65	88.0	.71	.555
.5	1028.8	1.5	1.6	86.8	.65	.51
.4	1027.7	1.35	1.42	81.6	.58	.30
.3	1027.3	1.28	1.6	86.8	.55	.555
.2	1031.0	1.83	1.2	75.2	.785	.444
.1	1027.6	1.34	1.1	71.8	.975	.444

DATA SHEET XII

HOLE K

Zero = 1017.9; Bar. = 30.08; T = 87; p in 3" = 1.11';
p (static) in 3" = .20'.

Traverse	R	% H_2	Pitot	V	c/c_1	$\frac{V - V_2}{V_1 - V_2}$
2.9	1029.8	1.68	1.10	72.0		
2.8	1030.7	1.80	1.17	74.0		
2.7	1029.9	1.69	1.45	82.5		
2.6	1030.8	1.81	1.33	85.5		
2.5	1031.4	1.88	1.35	85.5		
2.4	1030.4	1.75	1.55	85.5		
2.3	1031.2	1.86	1.52	85.0		
2.2	1031.7	1.94	1.70	89.5		
2.1	1032.2	2.0	1.60	86.8		
2.0	1030.5	1.77	1.65	88.0		
1.9	1029.0	1.56	1.65	88.0		
1.8	1029.9	1.70	1.60	86.8		
1.7	1031.1	1.86	1.8	92.0		
1.6	1031.7	1.95	1.8	92.0		
1.5	1031.2	1.88	1.8	92.0		
1.4	1029.7	1.68	1.8	92.0		
1.3	1030.2	1.74	1.7	89.5		
1.2	1031.3	1.88	1.8	92.0		
1.1	1030.7	1.81	1.75	90.7		
1.0	1030.7	1.81	1.72	90.0		
.9	1030.9	1.83	1.63	88.0		
.8	1029.2	1.60	1.55	85.5		
.7	1030.0	1.73	1.55	85.5		
.6	1030.2	1.75	1.4	81.0		
.5	1028.7	1.53	1.4	81.0		
.4	1028.0	1.44	1.35	79.5		
.3	1027.8	1.40	1.30	78.0		
.2	1028.6	1.52	1.20	75.0		
.1	1029.0	1.57	.95	66.6		

DATA SHEET XIII

HOLE L

Zero = 1017.4; Bar. = 30.12; T = 86; Δp in 3" = 1.11';
p (static) in 3" = .22'.

Traverse	R	% H_2	Pitot	V	c/c1	$\frac{V - V_2}{V_1 - V_2}$
2.9	1028.0	1.43	1.07	71.0	.85	
2.8	1028.6	1.56	1.2	75.0	.9	
2.7	1028.6	1.56	1.4	81.2	.9	.376
2.6	1029.5	1.70	1.6	86.3	.97	.665
2.5	1029.1	1.62	1.7	89.3	.93	.80
2.4	1029.0	1.61	1.7	89.3	.925	.80
2.3	1029.1	1.62	1.7	89.3	.93	.80
2.2	1029.2	1.67	1.7	89.3	.96	.80
2.1	1029.5	1.72	1.7	89.3	.99	.80
2.0	1030.0	1.78	1.78	91.0		.88
1.9	1029.3	1.70	1.8	92.0	.97	.94
1.8	1029.3	1.70	1.75	90.3	.97	.85
1.7	1029.6	1.74	1.80	92.0	1.	.94
1.6	1029.6	1.74	1.80	92.0	1.	.94
1.5	1029.3	1.70	1.85	93.2	1.	1.
1.4	1029.6	1.74	1.73	90.0	1.	.83
1.3	1029.2	1.68	1.80	92.0	.965	.935
1.2	1029.3	1.72	1.78	91.0	.99	.88
1.1	1028.7	1.61	1.7	89.3	.925	.8
1.0	1028.8	1.63	1.7	89.3	.94	.8
.9	1028.7	1.61	1.6	86.8	.925	.665
.8	1029.0	1.67	1.5	84.0	.96	.52
.7	1028.6	1.61	1.4	81.3	.925	.38
.6	1028.6	1.61	1.4	81.3	.925	.38
.5	1027.7	1.50	1.35	79.5	.86	.285
.4	1029.2	1.72	1.30	78.0	.99	.21
.3	1027.5	1.48	1.05	70.2	.85	
.2	1027.0	1.40	.95	66.6	.80	
.1	1026.4	1.32	.65	55.0	.76	

APPENDIX C

REFERENCES

(1) Oelheim and Thacher, "Analysis of Turbulent Mixing in Gas Streams by Thermal Conductivity cell." thesis submitted for M. S., Mass. Inst. of Tech., 1945.

(2) Towle and Sherwood, "Eddy Diffusion." Industrial and Engineering Chemistry, Vol 31, page 457, April 1939.

(3) Squire and Trouncer, "Round Jets in a General Stream" R and M No. 1974 (7591) A.R.C. Technical Report.

(4) A.S.M.E. Power Test Codes, Part S, Chapter 4, July 1939, "Instruments and Apparatus."

(5) Sherwood, "The Theory of Gas Aosorption" Chapter 1, Mass. Inst. of Tech., 1931.

(6) Roberts, "The Theoretical Scattering of Smoke in a Turbulent Atmosphere" Proc. Royal Soc. A104, pp 640-654, 1923.

(7) Prandtl, "The Physics of Solids and Fluids," Part II. Blackie and Son. 1936.

(8) Bakhmeteff, "The Mechanics of Turbulent Flow." Princeton Univ. Press, 1936.

DATE DUE

AUG 31
8 SEP 69
BINDERY
17338

Thesis 11661
N3 Naymark
Turbulent mixing along
the boundaries of
parallel flow streams

8 SEP 69 17338

Thesis 11661
N3 Naymark
Turbulent mixing along the
boundaries of parallel flow
streams.

Library
U. S. Naval Postgraduate School
Monterey, California

BRITISH
GOLD LETTERING
AND
SMITH BINDERY

thesN3
Turbulent mixing along the boundaries of
3 2768 002 01772 5
DUDLEY KNOX LIBRARY